SAE INTERNATIONAL

ARTICLE INFO

Article ID: 12-08-03-0025

doi:10.4271/12-08-03-0025

Rating the Surrounding Vehicle-to-Everything Field, Based on Channel Utilization and Information Influence

Christoph Pilz,[1,2] Lukas Kuschnig,[2] Alina Steinberger,[1,2] Peter Sammer,[2] Esa Piri,[3] Christophe Couturier,[4] Thomas Neumayr,[2] Markus Schratter,[1,2] and Gerald Steinbauer-Wagner[1]

[1]*University of Technology Graz, Austria*
[2]*Virtual Vehicle Research GmbH, Austria*
[3]*Kaitotek Oy, Finland*
[4]*YoGoKo, France*

Abstract

Automated vehicles (AVs) can get additional information from infrastructure and other vehicles via vehicle-to-everything (V2X) communication. However, how can an AV decide if the surrounding V2X field can reliably provide qualitative, relevant, and trustworthy information? Related research analyzes V2X performance from various angles. However, not only are there identified open gaps in the analysis of loaded channels, but there has also not yet been an effort to design a lightweight metric for rating the quality of the surrounding V2X field. Hence, this work aims to close this existing performance measurement gap and develop a metric for rating the quality of the surrounding V2X field. This article first highlights the gaps identified in performance analysis before closing them with a dedicated measurement campaign. Next, it combines these findings with related research to design a straightforward V2X field rating metric. The resulting V2X field rating metric is a starting point for the AD system to decide if sensor information from the V2X field should be directly incorporated or handled with care.

History

Received: 30 Apr 2024
Revised: 11 Jul 2024
Accepted: 01 Oct 2024
e-Available: 22 Oct 2024

Keywords

Automated driving, Automated vehicles, Cooperative connected automated mobility, Cooperative intelligent transport systems, Vehicle to everything, AD, AV, CCAM, C-ITS, V2X

Citation

Pilz, C., Kuschnig, L., Steinberger, A., Sammer, P. et al., "Rating the Surrounding Vehicle-to-Everything Field, Based on Channel Utilization and Information Influence," *SAE Int. J. of CAV* 8(3):373–396, 2025, doi:10.4271/12-08-03-0025.

ISSN: 2574-0741
e-ISSN: 2574-075X

1. Introduction

Automated vehicles (AVs), infrastructure, and other traffic participants share pre-processed information as a core part of cooperative, connected, and automated mobility (CCAM). CCAM is a subdomain of intelligent transport systems (ITS). The information is thereby exchanged via vehicle-to-everything (V2X) communication channels. ITS-Stations (ITS-Ss) are ITSs capable of sending and receiving via V2X communication. ITS-Ss exchange different types of information with different levels of importance. Among others, there is (i) critical and simple information, such as decentralized environmental notification (DEN), i.e., a warning about a traffic jam via DEN Messages (DENMs) [1], (ii) simple information, such as ITS-S configurations for cooperative awareness (CA), i.e., ego position and size via CA Messages (CAMs) [2], and (iii) complex information, such as data of the surroundings for collective perception (CP), i.e., sensor information via CP Messages (CPMs) [3].

Generally speaking, information improves the perception of the environment. However, the information has to be correct, accurate, and timely. Correct, meaning secure [4, 5, 6, 7] and trustworthy [8, 9, 10, 11], to avoid overall data corruption by adversaries. Accurate means positionally accurate, such as analyzed in research for CPMs [12], but also free from false positives and negatives, which detection algorithms are prone to [13, 14, 15]. Timely, with enough time to react to, but also faster than onboard perception, as discussed by Pilz et al. [16]. From the system's perspective, having as much information as possible that can be classified as correct, accurate, and timely is desirable. However, all V2X technologies in the 5 GHz band are physically limited in capacity. Specifically, a high information flow will result in channel congestion. This results in a situation where channel access for low-priority traffic can be substantially delayed; the lowest-priority traffic can even experience starvation with much high-priority traffic [17, 18, 19, 20], as Pilz et al. [16] discussed. Decreasing channel load is a most prevalent topic in the CP community, where the flow of information is high. The community analyzes (i) methods to mitigate redundancy [21], (ii) methods to pack detected objects into one instead of multiple messages [22, 23], and (iii) methods to decide which objects might be necessary at all [24, 25, 26, 27].

Stepping further, having correct, accurate, and timely data cannot be guaranteed, depending on the circumstances. There may be only a few issues when V2X is used to increase the comfort of passengers, but problems arise when safety barriers are lifted [16]. The existing European legal situation dictates that the driver of a vehicle has to be in control of everyday situations, such as a child stepping out between vehicles in a city. The driver has to drive accordingly to prevent an accident. Hence, an AV has to guarantee the same safety with its onboard sensors. However, within specific CCAM scenarios, one could increase the speed or mobility of an AV if, for example, standstill vehicles or infrastructure increase the field of view (FoV). This could be in many scenarios, such as driving in foggy conditions, valet parking, or virtual towing. Consequently, this leads to the need for a metric for deciding when to allow dependency on the V2X channel.

This article addresses both the lack of data for loaded V2X channels and the lack of a metric to rate the surrounding V2X field. The lack of data is tackled by filling the gaps identified by Pilz et al. [16] with additional tests. These tests include the quality of service (QoS) of currently rolled-out ITSs in the 5 GHz band (ITSG5) and aim to complement simulations [17, 28, 29]. This article then addresses the lack of a metric by proposing a method to rate the surrounding V2X field. The metric will provide feedback for automated driving (AD) systems, with parameters such as information availability, channel load, and transmission quality. It will further provide extensibility for additional parameters, the possibility of being used for a live geo-grid calculation, or even artificial intelligence (AI)-assisted predictions of future connectivity developments.

The structure of this article continues by providing details on the method used to acquire additional data and to design the metric in Section 2. This work's core contribution is then split into Section 3, dealing with filling data gaps in the QoS analysis of V2X behavior, and Section 4, dealing with the now possible definition of the metric to rate the V2X field. The defined metric is then applied to demonstrate scenarios in Section 5. Section 6 then discusses the overall process and its limitations before Section 7 concludes this work.

2. Method for the Metric Design

This work aims to design an extendable metric to rate the V2X field, which requires several details. Not all of them are available from related research. At a baseline, there is a general overview of components necessary for CP, discussed by Pilz et al. [30], which was extended by Cui et al. [31]. Their work on principal components was followed up again by Pilz et al. [12, 16], who provided a detailed analysis of a state-of-the-art AD system, once from the perspective of delay [16] and once from the perspective of accuracy [12]. Those results are the primary input for the rating metric. However, Pilz et al. [12, 16] highlight gaps for loaded channels and the FoV extension. Following their work, this work also aims to fill these gaps to gain a better overall picture of the performance of V2X.

Hence, this work will at first focus on filling gaps identified for (i) the channel load, (ii) the delay behavior in loaded channels, and (iii) the extension of the FoV. The channel load and delay behavior evaluations are conducted

in the lab and the field to provide a constructive discussion basis and metric. The evaluations of the FoV are to provide a clearer picture of what V2X-as-a-sensor can provide in CA/CP scenarios and how V2X can increase the efficiency of V2X applications.

Next, the metric can be designed. It is aimed to be lightweight and extendable, allowing parallel calculations and live feedback of the surrounding V2X field. Pilz et al.'s performance know-how [12, 16] is combined with measurements from this work to design rating metrics for singular performance components. Finally, the performance components are put together in a single metric.

3. Part I: Filling Data Gaps

This first part aims to close important gaps identified by Pilz et al. [12, 16]. This includes a lack of data for loaded channels and an analysis of the FoV extension possible with V2X-as-a-sensor in CA/CP scenarios.

3.1. Method for Filling Data Gaps

This work uses lab and field tests to fill data gaps. The laboratory tests aim to provide a reference point for loaded channels. The field tests provide insight into the behavior with messages of higher complexity and communication behavior with bigger distances. The following sections provide details on how to close existing gaps for (i) the channel load, (ii) the delay behavior in loaded channels, and (iii) the extension of the FoV.

3.1.1. Laboratory QoS Tests The laboratory tests are designed to provide a reference point in a controlled environment. The QoS tests are conducted in a single room in the laboratory to mitigate influences from the environment as well as from the network of the AVs. The basic setup is shown in Figure 1. A minimum of 1 m distance separates the sender, receiver, and adversary senders, while the adversary senders are centered in between. The adversary senders are ITS-Ss that deliberately fill the channel with valid messages. Listed in the following are the test scenarios in the laboratory:

- Basic QoS: sender and receiver are active. The QoS is measured for the transmission. This provides the ground level of QoS that can be expected.
- Single ITS-S load: as Basic QoS, but an adversary loads the channel from 0 to 1300 Hz of messages in 10 Hz increments. This provides insight into the QoS reduction that a single adversary can cause.
- Multiple ITS-S load: as Basic QoS, but multiple ITS-Ss send messages with 600 Hz. Specifically, up to seven ITS-Ss are used iteratively, and each generates 600 Hz of V2X messages. This provides insight into the QoS of a low-loaded channel.

3.1.2. Field QoS Tests The field tests are set up around the Graz University of Technology campus. The basic setup is shown in Figure 2. The sender and receiver are street-legal AD Demonstrators (ADDs) of the Virtual Vehicle Research GmbH. In all QoS scenarios, one vehicle sends and the other receives. A third vehicle is centered between and carries the other ITS-Ss as adversary sender sources. Listed in the following are the QoS-related scenarios:

- Single ITS-S load: the ADDs are standing apart at distances of 10, 50, 100, 150, and 250 m. According to the standard, one ADD sends CAMs and CPMs, each with a 1–10 Hz frequency. In between, a third vehicle with an ITS-S fills the V2X channel with CAMs from 0 to 1300 Hz in 10 Hz intervals. This shows how much influence a single ITS-S can have on the channel.
- Multiple ITS-S load: as single ITS-S load, but in between, there is a vehicle with six ITS-Ss, each filling the V2X channel with 600 Hz of CAMs. This provides insight into the QoS of a channel fully loaded from a low number of ITS-Ss.

FIGURE 1 Laboratory setup of the V2X QoS tests. Two vehicleCAPTAINs (sender/receiver) exchange messages. Six vehicleCAPTAINs or the Y-Ghost system (adversaries) send messages to fill the channel depending on the scenario.

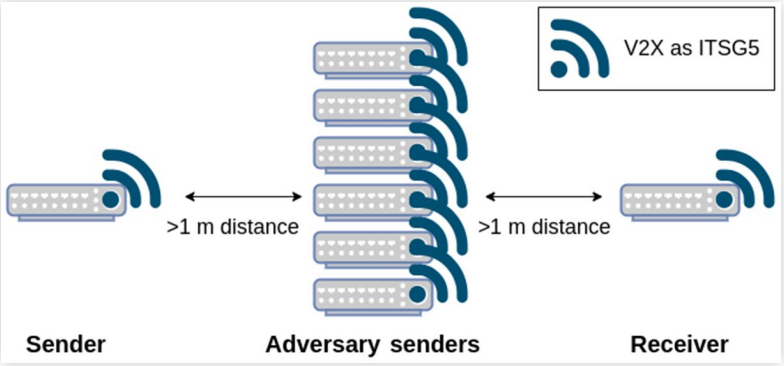

FIGURE 2 Field setup of the V2X QoS tests. Two vehicleCAPTAINs (sender/receiver) exchange messages. Six vehicleCAPTAINs or the Y-Ghost system (adversaries) send messages to fill the channel depending on the scenario.

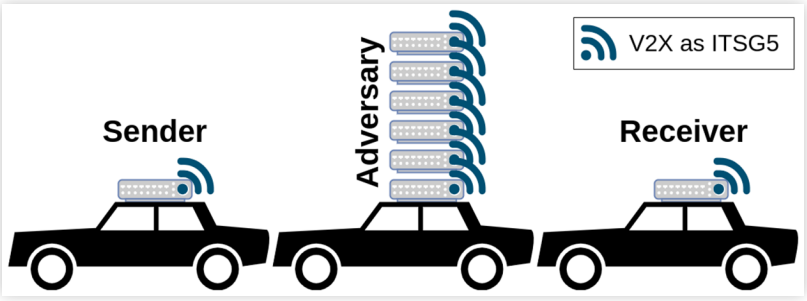

- Follower Scenario: is based on all previous scenarios concerning adversarial senders. All three vehicles drive at typical city distances around a 150 × 250 m building block. The adversary in-between runs the single ITS-S test for 0, 500, 1000, and 1300 Hz. The multiple ITS-S test is run with 2, 3, and 4 ITS-Ss. This provides insight into city scenarios with a loaded V2X channel.
- One-Corner Scenario: as single/multiple ITS-S load, but the second vehicle is standing across the corner, outside the FoV of the first vehicle. This should demonstrate a city corner scenario.

3.1.3. Field FoV Test The FoV field scenarios are tested at the Graz University of Technology campus. Selected are three basic CA/CP scenarios for AVs, as shown in Figure 3 and listed in the following:

- Follower Scenario: a classic follower example, where the leading vehicle extends the FoV of the follower.
- One-Corner Scenario: two vehicles can extend the FoV of each other, with an overlap at the intersection.
- No FoV overlap: the FoV of both vehicles do not overlap; hence, there is a 100% extension of the FoV. Additional CP-capable vehicles can extend the FoV even beyond the 100% increase.

3.2. Setup for Filling Data Gaps

The setup follows the architecture discussed by Pilz et al. [12, 16, 32, 33]. The following sections give a summary overview. Figure 4 shows the setup from a field operational perspective. The lab setup is without vehicles, i.e., communication only.

Describing the full setup, two street-legal ADDs are equipped with Autoware Universe, a state-of-the-art AD software stack. The AD software stack was adapted for the ADDs. The AD software stack was extended with the

FIGURE 3 FoV Test Scenarios. The ego vehicle (red) and another vehicle (blue) share perception information via CA/CP. Scenario I (t.l.) allows both vehicles to see each other. Scenario II (t.r.) allows both vehicles to share an overlap of their sensors. Scenario III (b.) allows only a V2X connection between the vehicles, but they do not share an overlapping FoV.

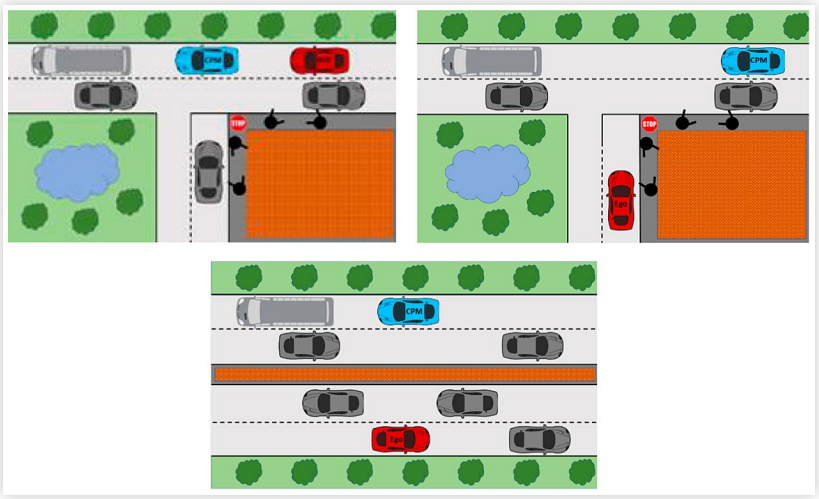

FIGURE 4 Basic test setup from field perspective (clockwise): the Autoware system provides CA/CP data. The V2X gateway prepares and sends the data via Ethernet to the vehicleCAPTAIN routing core, which arranges transmission via ITSG5. The Probe (Qosium) detects the packet when passing through the Ethernet interface. The receiving process is mirrored.

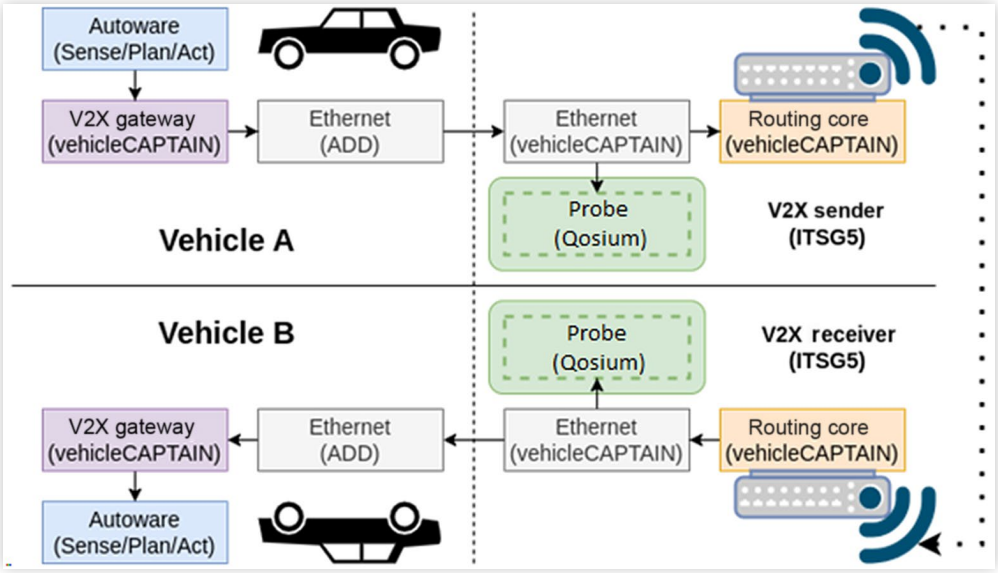

vehicleCAPTAIN toolbox, used as hardware and software components for V2X communication. The Qosium measurement suite is used to conduct and evaluate measurements for the QoS analysis. The Y-Ghost system controls iterative channel loading from a single ITS-S. Channel loading with multiple ITS-Ss is then done with seven vehicleCAPTAIN development kits. The final sections provide a few details necessary for reference toward the validity of results.

3.2.1. AD Demonstrators The setup of the ADDs is the same as in Pilz et al. [12, 16]. Similarly, a Ford Fusion and a Ford Mondeo are used, with street-legal hardware and software configuration, as shown in Table 1. The Virtual Vehicle Research GmbH provides both vehicles.

The vehicles are equipped with hardware and software, depending on the use case. Figure 5 shows the full sensor configuration of the Ford Fusion. The vehicle has four lidars: an Ouster OS2-128, three Ouster OS1-64, two FLIR Blackfly S Full-HD cameras, and six TierIV C1 cameras. For this work, only the single OS2-128 lidar for object detection was used to have a minimal test set without the multi-sensor setup as overhead. The processing software for this setup is discussed in Section 3.2.2.

The Ford Mondeo, also shown in Figure 5, has a dynamic sensor platform. This work uses a single Ouster OS2-128 lidar to detect objects. The information processing is similar to the software within the Ford Fusion, as discussed in Section 3.2.2.

TABLE 1 Hardware/software computing setup—automated driving demonstrators (ADDs).

Type	Ford Fusion	Ford Mondeo
CPU	Intel i7-9700k	Intel i7-11800H
GPU	Nvidia RTX 2070	Nvidia RTX 3070 Mobile/Max-Q
RAM	32 GB DDR4	32 GB DDR4
Software	Autoware	Autoware

3.2.2. Autoware Universe This work uses the Autoware Universe software stack as the basis. The stack was adapted for the ADDs and extended with CA/CP capability. Until now, the delay behavior [16] and its accuracy [12] have been validated. For this work, it is only important to recap that the CA information is created from onboard localization, and CP information is generated from objects detected by the lidar perception pipeline.

3.2.3. Qosium QoS Measurement Software This work employs a passive measurement solution, Qosium, to empirically evaluate the communications QoS for the V2X application. Qosium taps into the network traffic for measurements without interfering with the transmission and can measure the QoS for any IP or Ethernet-based application over any network technology in real-time, which allows it to conduct the measurements without modifying the communications system.

The measurement setup is end-to-end between two vehicleCAPTAINs, as shown in Figure 4. The Qosium measurement agent, Qosium Probe, is installed on the vehicleCAPTAIN platforms, and the measurement is carried out on their respective Ethernet interface instead of the V2X communications modules. The most emphasis in our analysis is put on one-way delay, jitter, message loss ratio, and message loss bursts, also considering the

FIGURE 5 The Ford Fusion (left) and the Ford Mondeo (right), each equipped with an Ouster OS2-128 (yellow circle) and V2X antennas (red arrow).

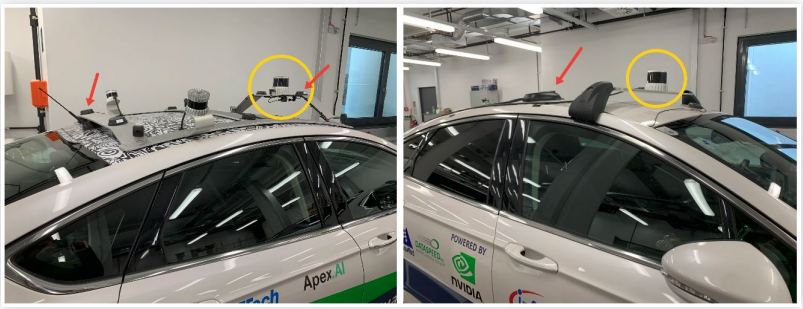

measured traffic statistics. The radio interface statistics, such as received signal strength indication (RSSI), were not collected in the experiments.

3.2.4. V2X Platform: vehicleCAPTAIN Toolbox The vehicleCAPTAIN toolbox is a collection of hardware and software components that allow easy access to V2X communication via multiple interfaces. Details of its features and the setup can be found in the respective Free and Open-Source Software (FOSS) repositories on GitHub [33]. The vehicleCAPTAIN development kit is the hardware part. A Raspberry Pi 4 8GB is the computing platform, and a Unex SOM301-E handles the ITSG5 communication. The controlling software, vehicleCAPTAIN routing core, handles the input/output relation between the Zero Message Queueing (ZMQ)-based Ethernet interface and the UnexSOM301-E for physical ITSG5 communication.

3.2.5. Y-Ghost Y-GHOST is a V2X simulation and emulation platform provided by YoGoKo. It is based on a Nexcom VTC-6210BK-embedded computer running under Debian 10 and equipped with an Atom E3845 processor at 1.91 GHz, 2 GB of RAM, and a Compex WLE200NX WiFi module configured for ITS-G5. This article uses two steps. In the first step, we record the CAMs sent at a rate of 10 Hz by each of the 130 simulated vehicles running in the same location as the real experiment. These records are then merged to generate 130 scenarios, each with a different number of cars ranging from 1 to 130. Then, in the second step, the scenarios are replayed to emulate the desired number of cars. This allows a controlled loading of the channel. Hence, the channel can be loaded from 0 to 1300 Hz worth of CAMs in 10 Hz increments. Note that for all tests performed with Y-GHOST, the signature of the messages at the Geo-networking layer is not activated.

3.2.6. Details: Adversary Senders For this work, adversary senders are used to load the V2X channel. As discussed in Section 3.1, this employs two different setups. First, a single ITS-S capable of iteratively loading the channel from 0 to 1300 Hz worth of CAMs in 10 Hz increments, based on the Y-Ghost system. This simulates a single adversary, filling the complete bandwidth. The mechanisms of ITSG5 are expected to easily handle this behavior.

Second, multiple ITS-Ss are used, each configured to send 600 Hz, based on the vehicleCAPTAIN. The frequency is lower, as the Unex Modules do not allow higher transmission rates. However, the goal is not to fill the bandwidth with a single adversary. The goal is to produce transmission collisions and trigger the channel maintenance algorithms of ITSG5 for high channel load.

3.2.7. Details: Localization Both vehicles use a lidar HD map for localization, as discussed in more detail in Pilz et al. [12]. This allows each vehicle to localize with a precision of less than 5 cm, with a combination of the lidar accuracy and the normal distributions transform Monte Carlo localization (NDT-MCL) algorithm provided by Saarinen et al. [34]. Summarized, a lidar HD map of the area is prerecorded. This lidar HD map is then equipped with a GNSS reference point. Both vehicles use this lidar HD map for localization. The lidar accuracy and the NDT-MCL combination allow localization of less than 5 cm for each vehicle in the same GNSS reference frame.

3.2.8. Details: Reference Time To provide accurate measurements for the time delays measured by the Qosium QoS software, the vehicleCAPTAIN development kits are synchronized via one pulse per second (1PPS) and chrony, as elaborated and validated in Pilz et al. [16]. The achieved synchronization with 1PPS is below 100 µs synchronicity. Summarized, the vehicleCAPTAIN development kit is equipped with a Ublox F9P module that allows integration of the 1PPS signal on the hardware level to the Raspberry Pi. This 1PPS trigger ensures a high precision clock of the hardware clock of the vehicleCAPTAIN development kit and, hence, a highly precise timing input for the Qosium QoS software.

3.2.9. Details: Transmitted Data Two vehicleCAPTAINs are used for communication in all setups. For the QoS tests, one sends and the other receives. The sender uses

a station ID <8000, and adversaries use a station ID >8000, which allows the vehicleCAPTAIN routing core to drop adversary packets to avoid causing a processing delay outside of the transmission delay. In the QoS laboratory tests, the vehicleCAPTAIN sends minimal CAMs with 41 bytes and ascending generation delta time to allow distinguishment between messages. In the QoS field tests, live CAM and CPM data are used from the sending ADD.

In the FoV field tests, vehicleCAPTAINs and their hosting ADDs are configured to send and receive CAMs and CPMs without purposefully placed adversaries.

3.2.10. Details: V2X QoS Measurement The measurement setup for the QoS of V2X is the same as that used by Pilz et al. [16]. The process can be explained as shown in Figure 4. Involved are two vehicleCAPTAINs. One is sending, and the other one is receiving. A message arrives at the Ethernet interface of vehicleCAPTAIN A. Here, the message is tracked by Probe A, which is the beginning of the QoS measurement. The message is then processed by the routing core of the vehicleCAPTAIN A and transmitted according to the ITSG5 standard. At the receiving end, the message is processed by vehicleCAPTAIN B and sent to the receiver via Ethernet. At the Ethernet interface, Probe B tracks the transferred message for real-time measurement of QoS statistics.

3.3. Measurements for Filling Data Gaps

The measurements are intended to provide missing QoS data for loaded V2X communication channels in the 5 GHz band, with the example of ITSG5. This section provides an overview of the results and highlights core findings.

3.3.1. Laboratory QoS Measurements The laboratory tests provide insight into the channel capacity and, in turn, message throughput performance, provided by the mechanisms carrier sense with multiple access with collision avoidance (CSMA/CA), enhanced distributed channel access (EDCA), and decentralized congestion control (DCC) [35]. The following paragraphs will discuss the basic QoS of V2X between two ITS-Ss, the channel behavior with a single adversary ITS-S, and the channel behavior with multiple adversary ITS-Ss.

3.3.1.1. Basic QoS. The performance of exchanging a simple 41-byte CAM with 10 Hz between two ITS-Ss has been demonstrated by Pilz et al. [16], which states 5 ms of expected transmission delay for small CAMs. This article provides a stronger baseline with a runtime of 1 h, with the V2X QoS measurement setup defined in Section 3.2. One can see from the data shown in Figure 6 that the delay is, on average, 4.99 ms, with well-distributed delay spikes of up to 19.46 ms, causing an average

FIGURE 6 Qosium QoS laboratory results averaged over 1000 ms for sending 10 Hz CAMs over 1 h. Stable channel reference.

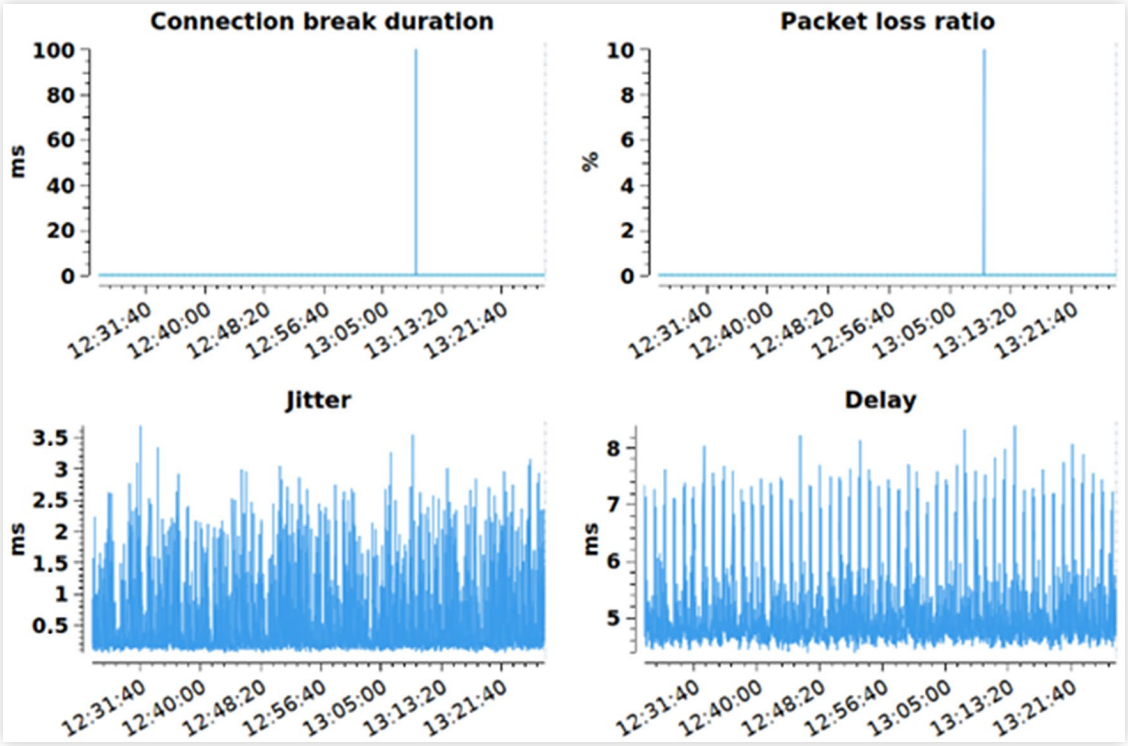

standard deviation (jitter) of 0.62 ms. This work also measured the connection break duration for connectivity and packet loss. Connection break duration is the time gap between two successfully transmitted packets when at least one packet is lost. For one lost packet, the connection break duration is 100 ms, i.e., one 10 Hz cycle. This is more visible in the other tests. Finally, after 1 h, there was only one lost packet.

3.3.1.2. Single Intelligent Transport System Station Load. The V2X channel capacity for ITSG5 can be calculated from specifications via the timeslots and message size. For a small CAM, the total channel capacity is close to 1400 Hz. To show the effects of a loaded channel, we configured the Y-Ghost system to send with a maximum frequency of 1300 Hz in 10 Hz increments. The overall time from 0 to 1300 Hz with 60 s for each 10 Hz iteration is 2 h 10 min. Hence, one can see the QoS in great detail, as shown in Figure 7. One has to remember that the Y-Ghost system is designed for basic sending, as discussed in Section 3.2. The CSMA/CA and EDCA mechanisms are kept simple and are designed for rapid sending. Hence, transmission from the vehicleCAPTAIN, with the fully activated CSMA/CA, EDCA, and DCC stack, struggles with lost packets. However, the packet loss is minimal, with an average of one lost packet in the 1000 ms averaging intervals. One can see that the packet loss is starting at around the first 10%. This is the time when the DCC mechanism dictates different channel behavior. However, the Y-Ghost system is designed to ignore the DCC mechanism, hence the packet loss, where the Unex module must adapt to the adversary. At around the 50% mark, the jitter starts to rise. This is the point where the channel gets slightly loaded. Later, the average delay also starts to rise. One can see that the vehicleCAPTAIN can still find gaps to transmit because the payload and frequency are only 41 bytes and 10 Hz, respectively.

3.3.1.3. Multiple Intelligent Transport System Station Load. The vehicleCAPTAIN utilizes the Unex SOM301-E modules for ITSG5 communication, as stated in Section 3.2. These modules are standard-compliant. Hence, one can evaluate the performance of the DCC algorithm with multiple senders. The DCC mechanism [35] generally requires a local minimum t_{off} = 25 ms, 40 Hz of maximum sending frequency. The total channel capacity is also limited to 160 Hz for messages without high-priority safety. This behavior is shown by the first test, shown in Figure 8. Here, 0–7 vehicleCAPTAINs send as many messages as possible, and another vehicleCAPTAIN is receiving. One can see that each added sender adds close to 40 Hz more messages until the 160 Hz of similar messages is reached. It is important to notice that the throughput will not increase as the DCC mechanism caps it. Hence, the sending vehicleCAPTAINs will suffer from substantially high channel occupancy, delaying transmission. The messages will not be lost, but the

FIGURE 7 Qosium QoS laboratory results averaged over 1000 ms for sending 0–1300 Hz worth of CAMs, in 10 Hz iterations, increasing every 60 s. The channel exponentially degrades.

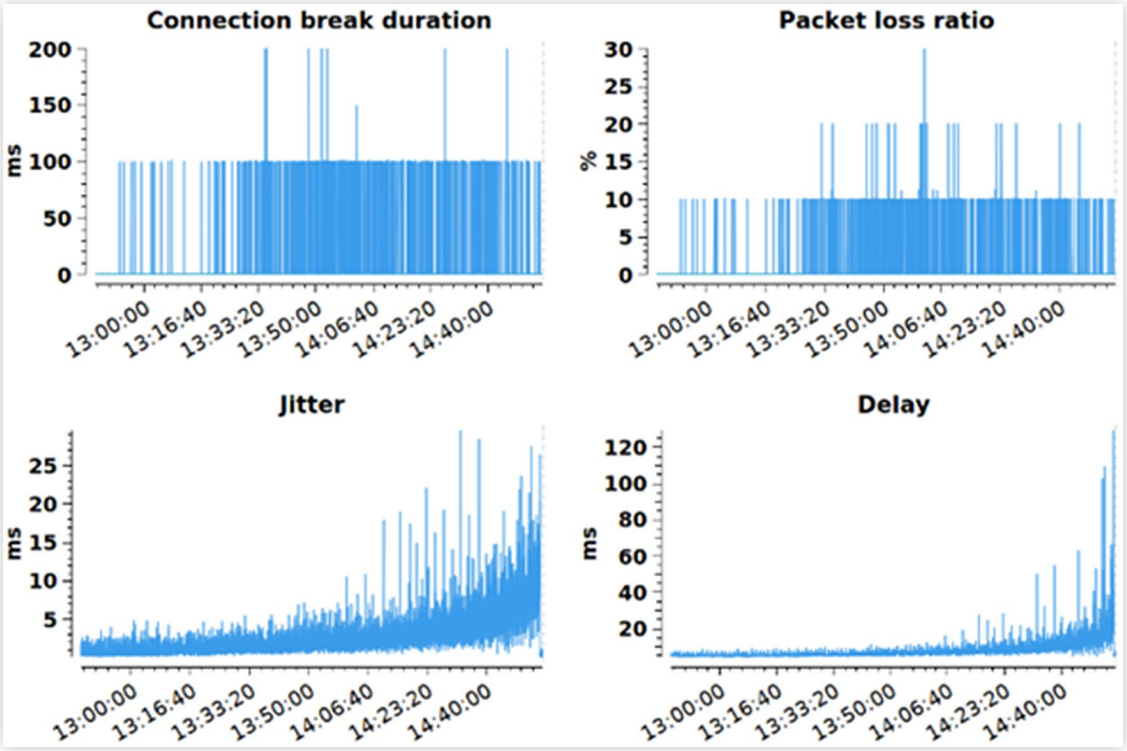

FIGURE 8 Laboratory: the x-axis shows the number of sending vehicleCAPTAINs. The y-axis shows the frequency received by another vehicleCAPTAIN. The left graph shows the frequency throughput with DCC = on. The right graph shows the frequency throughput with DCC = off. The V2X interface (Unex SOM301-E) configuration manages the DCC state. The channel starts degrading with the second adversary.

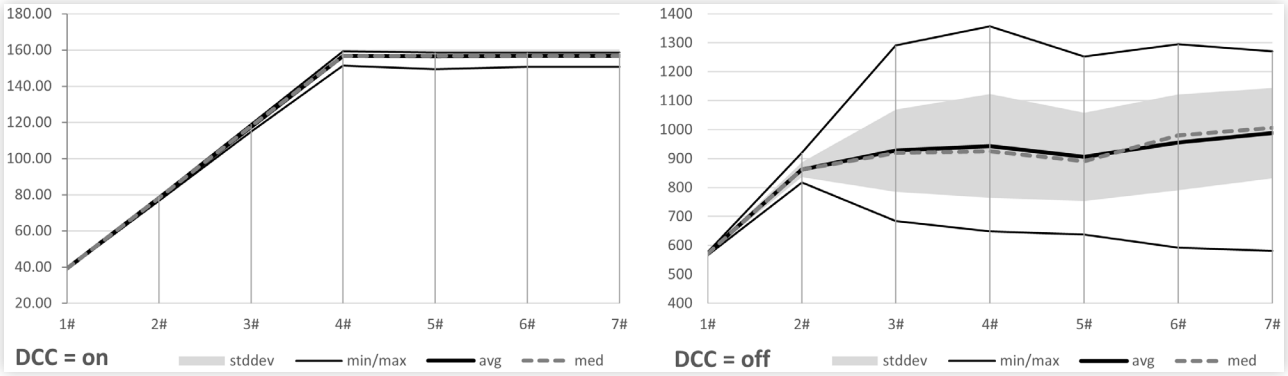

transmitting station waits for a silent channel for the back-off period counter and transmits the message.

The second test was done with a deactivated DCC mechanism, as shown on the right in Figure 8. Starting again with one vehicleCAPTAIN, one can see that the Unex SOM301-E tops out at around 570 Hz. One can also see the linear rise in maximum frequency when more vehicleCAPTAINs are added as senders. This maximum tops out at around 1300–1400 Hz, similar to the single ITS-S test before. The maximum frequency is not as stable as with the Y-Ghost system because more senders are involved, and the CSMA/CA and EDCA mechanisms regulate the channel. The channel regulation leads to an average throughput of 900–1000 Hz for the receiver. The average and median seem to climb slowly with more senders, which is expected, as the random-based channel management allows better throughput for the receiver. However, we cannot confirm this within the lab, as we would require more sender hardware.

The important fact is that while the receiver may have a constant flow of information, the messages are significantly delayed due to restricted channel access. The maximum throughput of the channel is reached, but the messages are stuck at the sender. However, this is only true for the involved adversary senders. If another ITS-S is added, the channel will still not be full due to CSMA/CA and EDCA. Proof can be given by the QoS measurements shown in Figure 9. Like the basic QoS test, one vehicleCAPTAIN sent 10 Hz worth of CAMs. Via a script, every 60 s, another vehicleCAPTAIN was started, trying to transmit 600 Hz worth of CAMs. Figure 9 shows that this is not noticeable for the two communicating vehicleCAPTAINs. However, this behavior can only be guaranteed with working CSMA/CA and EDCA mechanisms and the low amount of involved ITS-Ss.

Literature dealing with simulations, such as Shahen et al. [28], suggests that 10–20 ITS-Ss will create a noticeable delay. One hundred ITS-Ss will create around half a second delay due to limited channel access. It would be interesting to confirm those numbers with more ITS-Ss. But from our results, it seems plausible if one takes the 900–1000 Hz possible throughput.

3.3.2. Field QoS Measurements

All scenarios are designed to fill data gaps in the QoS in more fine-grained detail compared to previous approaches by Pilz et al. [16]. The focus is to extend the laboratory tests to fill data gaps involving distance and blocked lines of sight, as discussed in Section 3.1. Another difference is that for the field tests, live data is used for CAMs and CPMs, with standard conform generation frequencies, as discussed in Section 3.2.

3.3.2.1. Standstill Single Intelligent Transport System Station Load. The reference QoS measurements are taken at distances of 50, 100, 150, and 250 m. The Y-Ghost loads the channel with 0–1300 Hz worth of CAMs in 10 Hz increments every 10 s. The antennas are mounted on the roof of the ADDs and are not blocked by any other equipment in their line of sight. However, vehicles and people passed the line of sight within the 22-min runtime, causing delay and packet loss spikes.

The diagrams in Figure 10 show 100 m distance scenario. The packet loss ratio (PLR) is 6.3%, with an average delay of 15.2 ms and an average standard deviation (jitter) of 8.3 ms. One can also see that the effect of the channel loading is not as drastically visible as within the lab environment. However, the raw sending mode of the Y-Ghost system drastically causes a higher average delay and more packet loss, especially with delivery trucks moving in and out of the line of sight, which also causes more dynamic wireless reflections overall. It is also noteworthy that the delay goes down in the first 5% due to the moderation of the channel by the adversary as an active sender.

The distances of 0 and 50 m performed better than the 100 m scenario and were closer to the laboratory test results. On the other hand, toward 150 and 250 m, the

FIGURE 9 Qosium QoS laboratory results averaged over 1000 ms for 10 Hz CAMs, with 0–7 ITS-S adversaries added in 60 s intervals to the channel. The channel is stable.

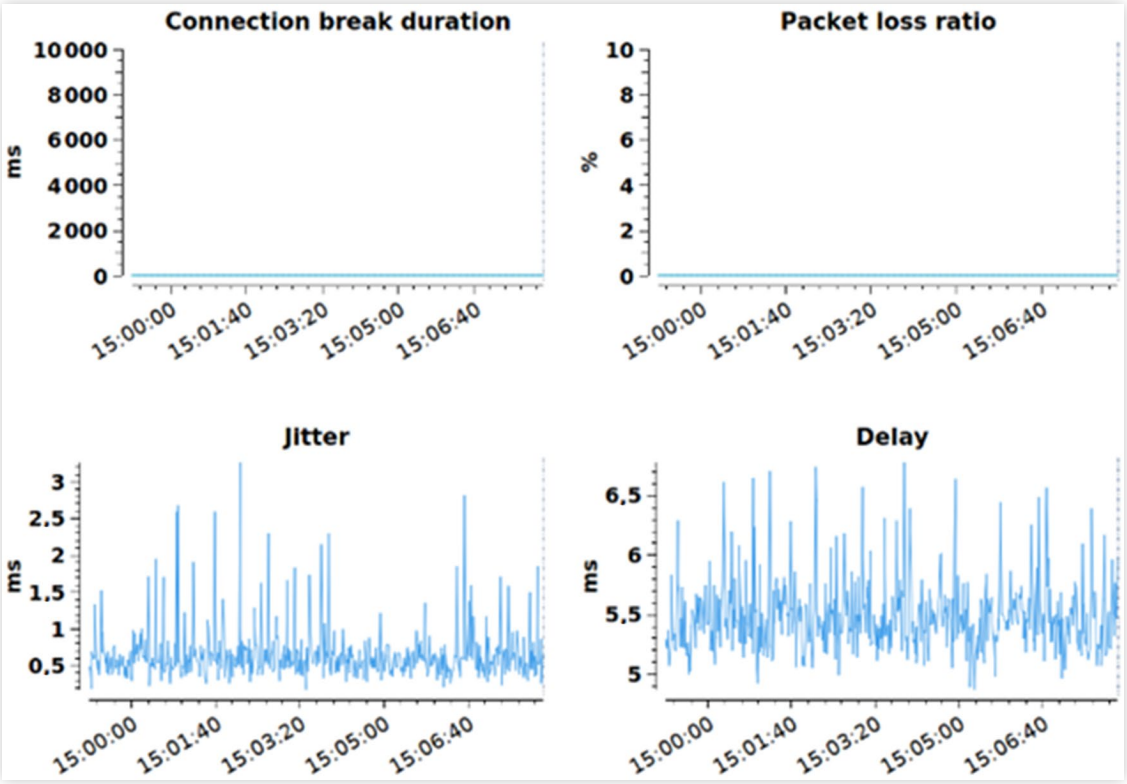

channel is increasingly disrupted by the raw sending mode of the Y-Ghost system, which causes an overall loss in maximum distance compared to research [16]. Specifically, while 150 m is only slightly worse with 23.7% PLR, 250 m already has 82.6% PLR.

3.3.2.2. Standstill Multiple Intelligent Transport System Station Load. The major difference to the laboratory test is the configuration of the payload. In this scenario, we use standard-compliant generation of CAMs and CPMs. Specifically, CAMs are generated with 1 Hz during standstill, and CPMs are generated with 1–10 Hz depending on the movement of vehicles and pedestrians. The campus road was busy, so the average CPM sending rate was 6–8 Hz. However, CPMs are much bigger than CAMs. While the CAM in the ADD has a payload of 64 bytes, the CPM has around 350 bytes. This is also visible in the tests. The 41-byte CAM in the laboratory setting could be easily transmitted. With nearly 10 times larger messages, the CPM in the field scenario suffers from increased transmission delays.

In the field test, the two vehicleCAPTAINs in the ADDs were configured to use a standard-compliant transmission with DCC = on, as within the lab. Six additional vehicleCAPTAINs were configured with DCC = off to support the maximum amount of sending frequency. A script was timed to start those, ramping from 0 to 6 adversary senders, with a step every 2 min. The result is an artificially loaded channel. While only having six ITS-Ss, the message load starves the transmission between the communicating ADDs, as shown in Figure 11. The delay and packet loss are low for 0–1 adversary senders. The delay jumps to around 50 ms, beginning with the second adversary sender, as the channel is full, as discussed in Section 3.1.1. Increasing the number of adversary senders furthermore increases the delay and the PLR.

We repeated these tests with increased distances, which showed results similar to those of the single ITS-S adversary. Specifically, the channel is loaded, which causes the maximum transmission distance to decrease rapidly.

3.3.2.3. Follower Scenario. The movement of vehicles with added adversary senders did not create any different result than adding adversary senders at a standstill or changing the distance. The distance between vehicles was <100 m for all three vehicles in the follower scenario, a typical city scenario of three vehicles. The result is a simple overlap of varying distances and interference, as shown in research [16].

3.3.2.4. One-Corner Scenario. For the one-corner scenario, the explanation is the same as for the follower scenario. The corner is a simple obstruction of the line of sight for wireless communication. This obstruction decreases the QoS, similar to increased transmission distances.

FIGURE 10 Qosium QoS field results averaged over 1000 ms for 0–1300 Hz adversary CAMs from the Y-Ghost system with 10 Hz iterations every 10 s. Distance 100 m. The channel degrades from the perspective of packet loss.

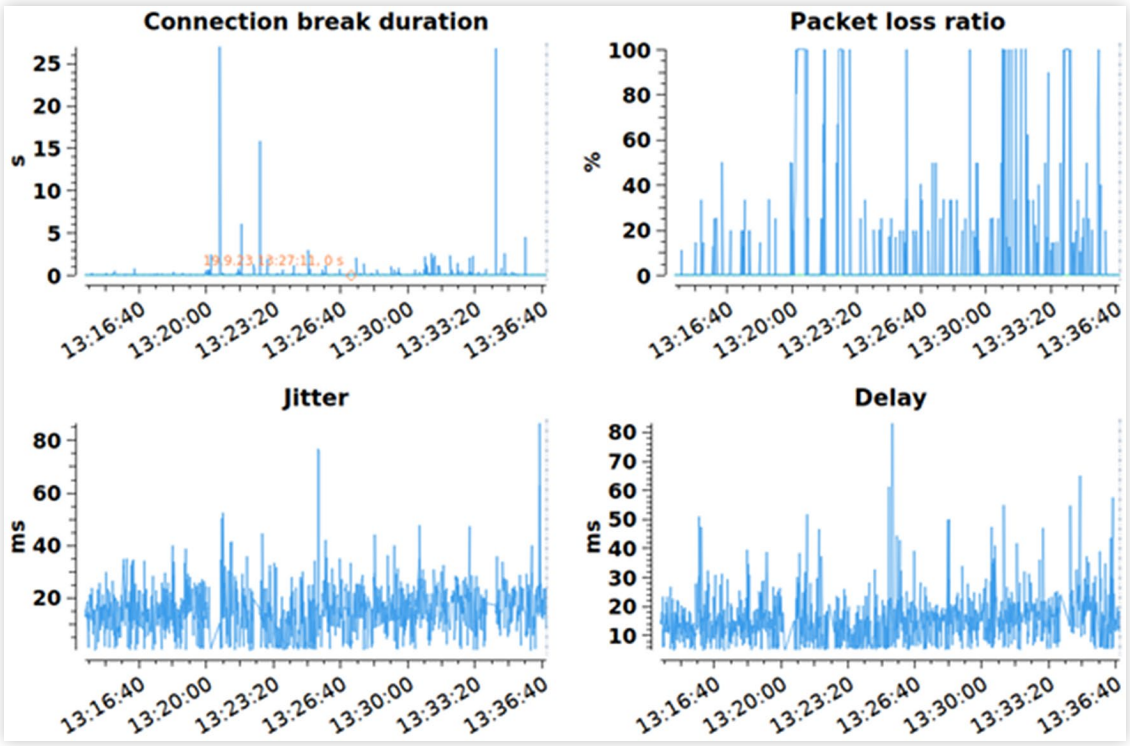

FIGURE 11 Qosium QoS field results averaged over 1000 ms for the full CA/CP stack in a side-by-side scenario, with 0–6 ITS-S adversaries added to the channel in 120 s intervals. The channel degrades beginning with the second adversary.

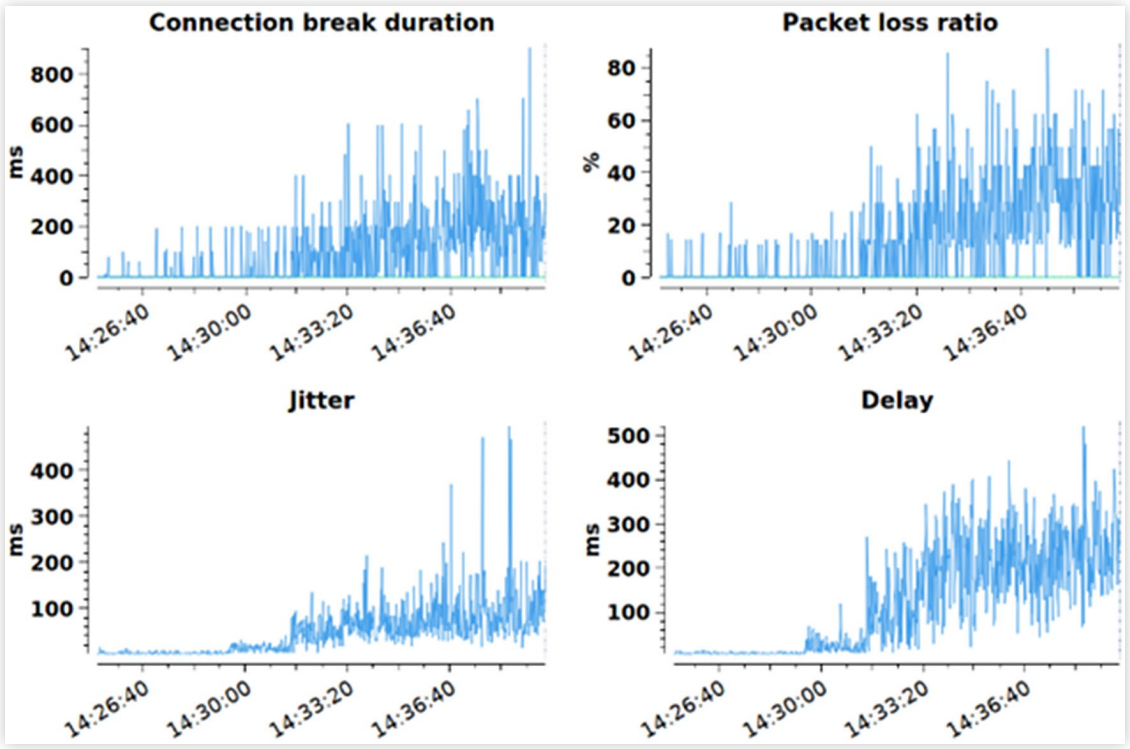

3.3.3. Field FoV Measurements The big advantage of V2X-as-a-sensor is the extension of the FoV. One can know about a situation without being able to detect it with onboard sensors. This can be best visualized by the three scenarios of the FoV field tests, as shown in Figure 12. From top to bottom, there is, at first, the side-by-side scenario. Two vehicles are roughly in the same position, standing beside each other. The FoV is just blocked by the other vehicle. In our tests, the ego vehicle (ADD: Ford Mondeo) detects, on average, 11 objects during the 5-min recording. The other vehicle (ADD: Ford Fusion) detects, on average, 13 objects. The number of objects detected by both vehicles is 8, whereas 3 objects were only detected by the ego vehicle, and 5 were detected by the other vehicle. From the perspective of the number of detected objects, this leads to an average increase of 45% for the ego vehicle.

The scenario in the middle is the one-corner scenario. The FoV overlaps at the intersection and, because of the shape of the intersection, also toward the bottom left corner. During the 5-min measurement period, the ego vehicle detected, on average, 8 objects and the other vehicle 6 objects. On average, 2 objects were detected by both vehicles, whereas 3 were detected by the ego vehicle and 5 by the other vehicle. From the perspective of the number of detected objects, this leads to an average increase of 62% for the ego vehicle.

The scenario on the bottom is the no-overlap scenario, where a row of bushes separates the ego and the other vehicle. The FoV is extended close to 100% by one vehicle, as the overlap of sensor ranges is minimal. During the 5-min measurement period, the ego vehicle detected 8 objects and the other 12 objects. On average, there was 1 object detected by both vehicles. From the perspective of the number of detected objects, this leads to an average increase of 137% on the ego vehicle side. If one puts more than one ITS-S with CPM capability, the FoV, and thus, the number of detected objects could be extended even further.

However, while those measurements indicate the benefit of detectable objects, two major questions must be examined. The first one is about the importance of free space. The sensors of an AV allow the declaration of free space around the vehicle simply by assuming that the space between an object and a sensor is free. The CPM is prepared for this, as it allows the inclusion of sensor configurations. However, this is not the case for CAMs or other message types. This allows the receiving ITS-S to know what is there, but except for the CPM, the recipient does know few things about the free space.

The second question concerns sensor coverage in general. A message, such as a DENM, may provide a simple status and may not provide spatial coverage, while a CAM tells something about the occupation of the space defined by length and width. Only the CPM can provide coverage information with objects and free space. Yet again, not much is known about how far an area the sensor can cover, which is a general problem in the robotics domain.

3.3.4. Summary of Findings The measurements are designed to cover a broad spectrum. The most important key findings are shown in Table 2. The laboratory tests focused on the channel's basic performance to foster comparability with related research and provide insight into channel maintenance methods, such as CSMA/CA, EDCA, and DCC.

The field tests start with a side-by-side setup similar to the lab setup to allow comparison of results. Then, they are extended with distance-dependent scenarios. Finally, the field FoV tests provide insight into the FoV increase with CA/CP data and raise questions about missing information on free space, occupancy, and overall sensor coverage.

4. Part II: Metric Design

The metric is based on QoS parameters collected by Pilz et al. [12, 16], extended by findings discussed in Section 3. The combined set contains the most basic parameters to describe the QoS of the surrounding V2X field. The input parameters themselves are complex. However, this complexity can be reduced easily due to the input features.

Figure 13 shows the components considered for this first draft. Each component and its metric will be discussed in the following sections. It is important to note that this list is not considered exhaustive and focuses on the 5 GHz band, specifically ITSG5. Other forms of V2X communication, such as mmWave or mobile networks with server backends, need different metrics and, in part, different rating parameters.

Overall, the metric should provide a rating for the current state of the V2X field as a sensor source, between 0 and 5, as defined by Equation 1. Key factors are (i) the channel load, (ii) the quality of information, (iii) the relevance of information, and (iv) the trustworthiness of information.

$$R \in \mathbb{N}\left[0,5\right] \qquad \text{Eq. (1)}$$

To foster relatability, the rating is mapped to denotations, as shown in Table 3. This table briefly explains what to expect from a specific rating, comparing onboard perception to information from the surrounding V2X field.

Finally, each component and their respective subcomponents are equipped with an influence weight ω, which is intended to be set implementation-specific and situation-specific. Implementation-specific means fitting the AD stack and its inherent planning process. Situation-specific means that different use cases require different quality features.

FIGURE 12 FoV scenarios are side-by-side following (top), around one corner (middle), and split by a row of bushes (bottom). The ego (gray) vehicle (yellow arrow) uses the lidar to detect object bounding boxes (green). A second vehicle sends a CAM (orange) as its position and its detected object bounding boxes via CPMs (blue).

TABLE 2 Key findings of the measurements.

Test scenario	Key finding
Lab QoS basic	Baseline 4.99 ms average delay and 0.62 ms jitter.
Lab QoS single adversary (single ITS-S 1300 Hz CAMs)	PLR rises to 10%, and the delay to 25–30 ms.
Lab QoS multiple adversaries (multiple ITS-Ss 600 Hz CAMs)	Channel load comparison with DCC = on/off. CSMA/CA and EDCA work when the channel is completely loaded with multiple ITS-Ss.
Field QoS standstill basic	
Field QoS standstill single adversary	Distance increases delay and jitter (+10 ms). Distance increases PLR up to 82.6% at 250 m. PLR indicates that distance effects on delay and PLR are caused by fading signal strength in combination with background effects.*
Field QoS standstill multiple adversary	Six adversaries lead to an average delay of around 250 ms, an average jitter of around 100 ms, and an average delay of around 30%. Signal strength and background effects* are likely causing this big difference in the field.
Field QoS follower scenarios	Results overlap with fixed standstill distances.
Field QoS corner scenario	Results are an overlap to high distances.
Field FoV scenarios	FoV increase can be shown for objects. Tests raise questions about occupancy. Tests raise questions about sensor coverage.

* Background effects may include, among others, signal reflections and other wireless noise.

FIGURE 13 Components of the metric rating the V2X field.

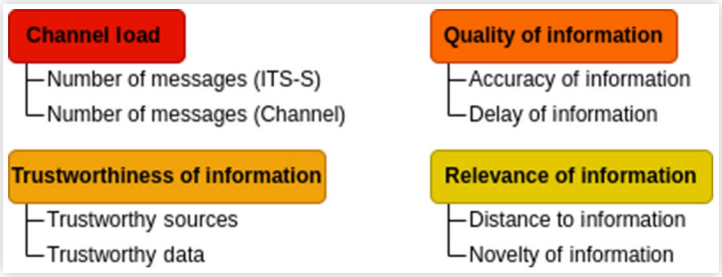

TABLE 3 Rating levels of the V2X field.

Rating	Denotation	Explanation
0	N/A	Not available or not considered
1	Sparse	There is useful information from time to time
2	Bad	There is useful information, but not always
3	Okay	The FoV can be extended
4	Good	Information as useful as onboard information
5	Excellent	Information better than onboard information

4.1. Channel Load

The channel load rating R_{CL} involves two components: the capacity of single ITS-Ss $R_{CL(msgs,its)}$ and the overall channel capacity $R_{CL(msgs,ch)}$, both shown in Figure 14. The overall R_{CL}, shown in Equation 2, is the weighted sum of the N_{itss} individual channel loads and the overall channel load. The weights $\omega_{CL(itss)}$ and $\omega_{CL(ch)}$ depend on the AD system and the driving situation. The following paragraphs will describe their features in more depth.

$$R_{CL} = \frac{\left(N_{itss}^{-1} * \sum R_{CL_{msg,itss}}\right)\omega_{CL_{itss}} + R_{CL_{msgs,ch}}\omega_{CL_{ch}}}{\omega_{CL_{itss}} + \omega_{CL_{ch}}} \quad \text{Eq. (2)}$$

4.1.1. Number of Incoming Messages per Station

Section 3.3 showed that individual ITS-Ss suffer starvation if the message frequency is too high. Specifically, the DCC manages the limit via the channel busy ratio (CBR). Depending on the available number of messages on the channel, the DCC dictates the t_{off} and, therefore, the maximum frequency for sending. This results in 0–40 Hz for a single ITS-S and 160 Hz for multiple ITS-Ss, as shown in Section 3.3.

The capacity of a single ITS-S can be seen parabolic, as shown in Figure 14. The best setup is exactly in the middle. There are enough messages from one station to have a consistent flow of information, but there is still room for additional messages. The components for this parabolic rating are shown in Equation 3. The range for x is from 0 to DCC_{max}, with DCC_{max} being dictated by the CBR in the DCC mechanism. The value r is the number of rating steps.

$$R_{CL_{msg,itss}} = \frac{\left(\frac{DCC_{max}}{2}\right)^2 - \left(\frac{DCC_{max}}{2} - x\right)^2}{\frac{1}{r}\left(\frac{DCC_{max}}{2}\right)^2} \quad \text{Eq. (3)}$$

4.1.2. Number of Incoming Messages per Channel

Reaching beyond the DCC, the channel capacity dictates the upper limit. For small CAMs, and therefore small emergency DENMs, this is around 1300 Hz for single ITS-Ss and, on average, around 1000 Hz for multiple ITS-Ss. However, the latter is very uncertain, as discussed in Section 3.3.

From a channel perspective, it is better to have fewer messages, as an unloaded channel allows individuals to send information. Hence, the more messages there are, the worse the channel quality, as shown in Figure 14. The rating $R_{CL(msgs,\,ch)}$, shown in Equation 4, can be calculated for x from 0 to N, with N being the maximum number of messages expected in the channel and σ being a tuning parameter. In our example, we selected N = 1300 from the Y-Ghost tests and σ = 2 to reflect the uncertainty shown in the multi-sender approach. Both numbers can be adapted to expected message sizes and channel capacity.

$$R_{CL_{msgs,ch}} = r * e^{-\frac{\sigma}{N} * x} \quad \text{Eq. (4)}$$

4.2. Quality of Information

The quality of information rating R_{QI} can be calculated as shown in Equation 5. Pilz et al. [12, 16] have discussed its elements, the accuracy, and age of information, shown in Figure 15, in great detail. The V2X message system can already check accuracy and age if the respective fields are filled out in the V2X message. If the fields have not been filled out or there is doubt about the data, this has to be analyzed in the trustworthiness rating.

$$R_{QI} = \frac{\omega_{QI_{acc}} R_{QI_{acc}} + \omega_{QI_{age}} R_{QI_{age}}}{\omega_{QI_{acc}} + \omega_{QI_{age}}} \quad \text{Eq. (5)}$$

FIGURE 14 Channel load metrics for the V2X field rating metric. Messages per incoming ITS-S (left). Load of messages on the channel (right).

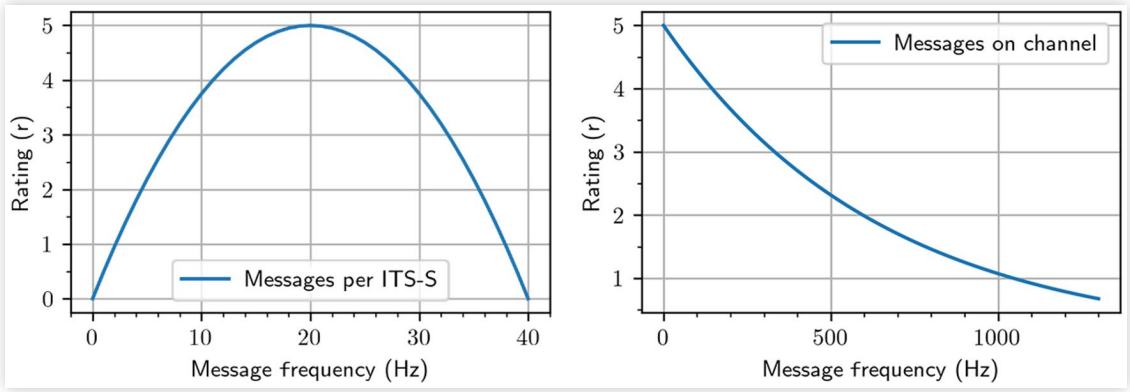

FIGURE 15 Quality of information metrics for the V2X field rating metric. Accuracy of information (left). Age of information (right).

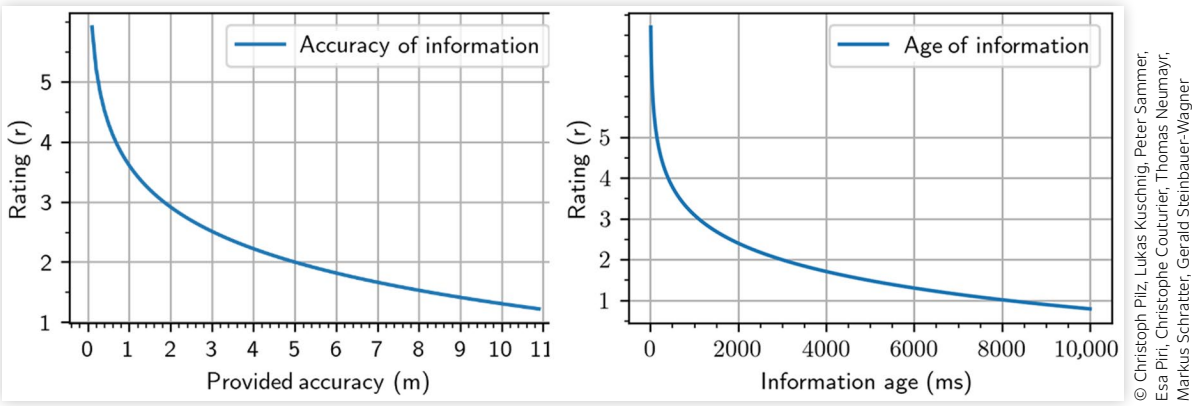

4.2.1. Accuracy of Information Ground truth is the best and can be provided for speed limits, intersections, and construction sites. However, localization of vehicles is already off due to sensor accuracy. Pilz et al. [12] expect an accuracy of 2.5 cm for the localization. Reid et al. [36] state localization requirements of 0.2–1.4 m and 0.1–0.29 m for highways and cities, respectively. However, while the input for CAMs is localization, this differs from other events detected with sensors, such as for CPMs or DENMs. Pilz et al. [12] expected an accuracy of 2.5–8 cm for the distance accuracy of a lidar sensor. Including point cloud filtering and object detection, the accuracy can be expected to be around 10 cm for the side facing the ego vehicle. Depending on the objects' shape, uncertainty can be higher than 1 m in the depth information. For CPMs, generally, one can expect an accuracy of around 0.3–1.9 m for standstill and low speeds. Hence, the accuracy of information $R_{QI(acc)}$, shown in Equation 6, is highest below 0.1 m. After that, it will rapidly decrease to a minimum of around 10 m, as shown in Figure 15. Finally, if the accuracy is ground truth, i.e., with x = 0, the $R_{QI(acc)}$ = 5, which conforms to the best rating.

$$R_{QI_{acc}} = 2 - \ln\left(\frac{x}{5}\right) \quad \text{for } x > 0 \qquad \text{Eq. (6)}$$

4.2.2. Age of Information The rating for the age of information $R_{QI(age)}$ is based on the time from an event happening until the knowledge has arrived, as discussed by Yates et al. [37]. For V2X, this has been shown by Pilz et al. [16]. This is especially important when dealing with CPMs, for example. CPMs may be sent out immediately for critical data. However, the frequency may be lower than the 10 Hz cycle for load protection and less important data. Yet, a loaded channel already means a bad rating on R_{CL}, so penalizing both satisfies the metric.

We take everything <100 ms as excellent for the metric, following Pilz et al. [16]. This equals information, such as the localization in a CAM, or permanent information, like construction sites within a 10 Hz cycle. 1 s old information is okay because it fits into 1 Hz cycles. Finally, everything older than 10 s should be considered aged and probably irrelevant.

Equation 7 shows the resulting $R_{QI(age)}$, which is calculated using a half-life-like time formula, as shown in Figure 15. For information without delay, i.e., x = 0, the $R_{QI(age)}$ = 5, which conforms to the best rating.

$$R_{QI_{age}} = 10 - \ln(x) \quad \text{for } x > 0 \qquad \text{Eq. (7)}$$

4.3. Relevance of Information

Equation 8 shows that the rating for the relevance of information R_{RI} is distance-dependent and novelty-dependent. Figure 16 shows the input shape of the components, which are discussed in further detail in the sections below.

$$R_{RI} = \frac{\omega_{RI_{dist}} R_{RI_{dist}} + \omega_{RI_{novel}} R_{RI_{novel}}}{\omega_{RI_{dist}} + \omega_{RI_{novel}}} \qquad \text{Eq. (8)}$$

4.3.1. Distance of Information There are two approaches to rating the distance of information $R_{RI(dist)}$. The first approach is rating the maximum sending distance, which was discussed in depth by Pilz et al. [16]. From a top-level perspective, the channel load handles the maximum sending distance, as explained in previous sections. Specifically, the maximum sending distance depends on the transmission power and the messages that can be received. Hence, the approach used for the metric is rating the distance of the sent content. The geographical networking (GN) layer allows the distribution of messages outside the true geographical location and forwarding messages beyond the true geographical location. All, of course, within the specified geographical validity.

For $R_{RI(dist)}$, shown in Equation 9, we rate the distance between the location of the ego ITS-S at the time of reception and the event's location. In the case of messages

FIGURE 16 Relevance of Information metrics for the V2X field rating metric. Distance of information (left). Novelty of information (right).

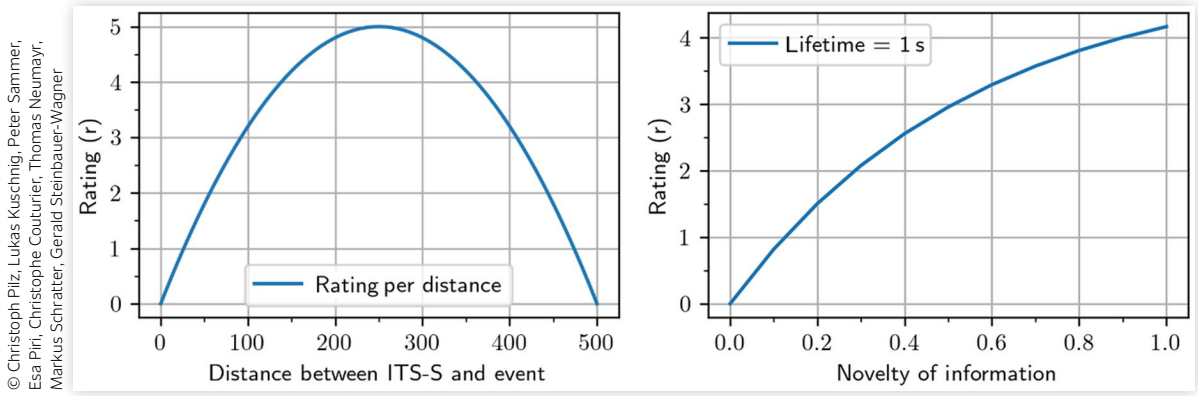

with multiple events, such as with multiple objects in CPMs, the target location is the location of the central element, in this case the central reference, i.e., ego vehicle or RSU. We expect a parabolic-shaped rating, with 250 m having the best rating, as this is beyond the FoV of most used sensors but still close enough to be relevant for most driving scenarios. Closer distances cross the 100 m mark, where we receive information already available with local sensors, as discussed by Pilz et al. [12]. Conversely, information farther away than 400 m may change until the ego vehicle is close. For example, highway speeds are too fast for such distant information to be highly relevant, and in cities with low speeds, information may change or be detected by onboard sensors way in advance.

$$R_{RI_{dist}} = \frac{\left(\frac{range_{max}}{2}\right)^2 - \left(\frac{range_{max}}{2} - x\right)^2}{\frac{1}{r}\left(\frac{range_{max}}{2}\right)^2} \quad \text{Eq. (9)}$$

4.3.2. Novelty of Information The AD stack uses information for planning that must be available within specific periods. Reaction time for operational planning is around 100 ms, path planning takes around 1 s, and mission planning can be >10 s, as discussed by Pilz et al. [16]. The complement is true for input data. Sensor data, such as the exact positions of pedestrians on the road, should have a maximum estimated lifetime of 100 ms because movement prediction will be difficult. The end of a traffic jam is 1 s because of additional oncoming vehicles. The location of a construction site or speed limit is >10 s because it's persistent. For our metric, we rate the existing information to have five half-times for a five-star rating. The novelty of information rating $R_{RI(novel)}$ for new information is r = 5, the highest rating level. For existing information, t is the current lifetime, and t_{max} = [0.1, 1, 10] the maximum lifetime validity, as shown in Equation 10. Therefore, the plot for repeated information would have the shape shown in Figure 16.

$$R_{RI_{novel}} = r - \left(r * e^{-\ln(r+1)\frac{t}{t_{max}}}\right) \quad \text{Eq. (10)}$$

4.4. Trustworthiness of Information

Trustworthiness is a matter of security and data correctness. Security is mainly concerned with protecting the V2X channel against adversaries. Data correctness deals with verifying data that does not have malicious intent. Trustworthiness of information R_{TI} is the sum of trustworthy sources and the available, trustworthy data, as shown in Equation 11 and Figure 17.

$$R_{TI} = \frac{\omega_{TI_{srcs}} R_{TI_{srcs}} + \omega_{TI_{data}} R_{TI_{data}}}{\omega_{TI_{srcs}} + \omega_{TI_{data}}} \quad \text{Eq. (11)}$$

4.4.1. Trustworthy Sources The rating of trustworthy sources $R_{TI(srcs)}$ indicates the trustworthiness of data from ITS-Ss. We expect a Gaussian distribution of the trustworthy ratings for each source. The ratings for a single source can be sampled, as shown in Equation 12 and Figure 17. A rating of three is a basic trust via certified sources. Toward a rating of one, there is distrust with ITS-Ss that it cannot provide enough security. Toward a rating of five, we have ITS-Ss verified using additional V2X security. Generally, the rating of trustworthy sources results from ongoing research in V2X cyber security challenges, ranging from attacks on the ITS backend [4] and on the certification system [5] over classical network attacks on the communication [5] straight to transmission of data with malicious intent [7]. The main goal of trustworthiness in V2X is to ensure mutual trust between

FIGURE 17 Relevance of information metrics for the V2X field rating metric. Trustworthy sources (left). Trustworthy data (right).

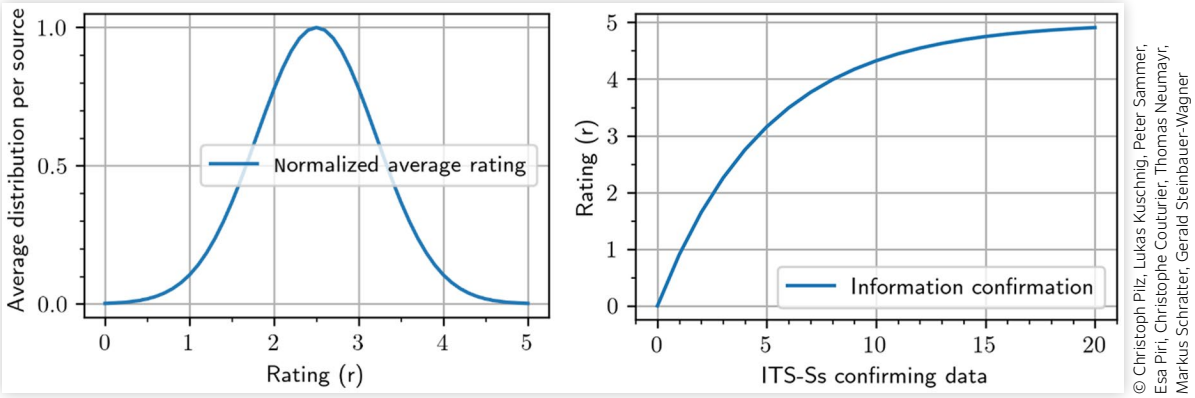

communication partners, either created through a peer network or assisted by central backends.

$$\text{Expected } R_{TI_{srcs}} \text{ distribution} = e^{-(r-2.5)^2} \qquad \text{Eq. (12)}$$

4.4.2. Trustworthy Data The rating on trustworthy data deals with the correctness of data [8, 9, 10, 11]. Specifically, incoming data may not necessarily be wrong due to malicious intent. Trustworthy sources can filter malicious intent. However, data may be wrong due to adverse weather, sensor malfunctions, or sending poorly localized ITS-Ss. Yet the information may still be valuable. One way to approach trustworthy data is cross-confirmation with other incoming sources. Similar to the onboard sensors of an AV. Hence, the trustworthy data rating $R_{TI(data)}$ is chosen to follow a saturation, increasing with the rate σ, as shown in Equation 13. For the plot shown in Figure 17, we chose $\sigma = 5$, as this fits well with the estimations of Zheng et al. [18] about the channel load causing issues with >20 vehicles. Figure 17 shows $R_{TI(data)}$ needing a good data confirmation set before saturating.

$$R_{RI_{itss}} = r\left(1 - e^{-\frac{x}{\sigma}}\right) \qquad \text{Eq. (13)}$$

4.5. FoV of Information

The FoV is not yet integrated into Figure 13 as a metric element, as it needs to be further analyzed and discussed. The measurements around the FoV extension revealed two core elements of the FoV. However, as the following discussion will show, they need some work before being integrated into a simple metric.

4.5.1. FoV Coverage The first element to rate the quality of the extended FoV is the sensor coverage. Specifically, what area is covered by the sensors of another ITS-S? Influencing factors for the metric are the sensor coverage itself. Speaking only of CPMs, the sensor coverage can be given by the parameters of the sensor setup that can be distributed with the CPM.

However, the sensor image contains blind spots due to obstructions. For a true picture of the sensor coverage, information must be provided by something, such as occupancy grids, which increases the effort in communication from high-level sensor data to feature-based data, as discussed by Pilz et al. [30]. Additionally, other messages, such as CAMs, may only provide information for a certain bounding box, or DENMs may only provide meta information of the area. How can we interpret the latter for FoV coverage?

To reveal another question, let one solution be that there is a message describing the FoV. The metric to rate the FoV coverage could then calculate the FoV increase by comparing the ego FoV with the FoV provided by other ITS-Ss, whereas the FoV of the other ITS-Ss has to be corrected for overlaps first. This method would raise two questions: (i) How should one handle the gaps between higher and lower quality between two FoV areas? and (ii) how should one handle the gap in trustworthiness between FoV areas?

Finally, how do we pinpoint the quality of the resulting FoV coverage? Where can it be put into the 0–5 rating scale? What is the difference between bad and good FoV coverage and excellent coverage?

4.5.2. FoV Occupancy The previous section indicated a need for this metric by discussing the differences between DENMs, CAMs, and CPMs. Section 1 introduced V2X-as-a-sensor by claiming that factual information may always increase one's perception of one's environment. However, the mentioned messages also primarily spread information that is there, but what is missing is information that is not there, most prominently free spaces.

The onboard sensors of an ego vehicle detect objects, and due to sensor placement and characteristics, they can also provide information about the surrounding free space. For example, if one takes a lidar, the space between

the sensor and the object is typically free. Exceptions apply, of course, if it is a mirror or similar optical effect.

This means, in turn, that much information for calculating the FoV occupancy may be missing. Occupancy calculations are, at their base, already computationally intensive. If there is an additional lack of information, the calculation may not benefit the system. Future research must analyze the domain of AD planners and occupancy grid calculation and compare them to the limited bandwidth and information gained through V2X.

4.6. Final V2X Field Rating

The final V2X field rating consists of all primary components, as shown in Equation 14, with weights ω_{CL}, ω_{QI}, ω_{RI}, ω_{TI} depending on the needs of the AD software and the driving situation. Specifically, slow driving scenarios in parking lots may require a higher focus on the distance of information to ensure the information is applicable. City driving scenarios may have more focus on the trustworthiness of information to avoid routing manipulation.

$$R = \frac{\omega_{CL}R_{CL} + \omega_{QI}R_{QI} + \omega_{RI}R_{RI} + \omega_{TI}R_{TI}}{\omega_{CL} + \omega_{QI} + \omega_{RI} + \omega_{TI}} \quad \text{Eq. (14)}$$

Finally, the metric design is deliberately lightweight and distributed to allow calculation with each received message. This allows the AD system to have rating information for each received dataset and to have a live report of the surrounding V2X field. This is also where the implementation-specific weights are important. For example, one monitoring application may use weights focused on trust and accuracy to provide insight into the actively received message. Another monitoring application may rate the average quality of the surrounding V2X field by channel load and age of information. This allows the estimation that emergency messages are highly likely to be put through the V2X network.

5. Metric Application

This section demonstrates the benefits of the rating metric defined in Section 4. The metric is applied to three different hypothetical scenarios. The scenarios are (i) a standard highway drive with low traffic, (ii) a big city scenario during rush hour, and (iii) a parking lot scenario at a mall. These scenarios will cover situations with low and high traffic, information density, and a specific use case scenario for V2X.

Table 4 provides the final expectations of the input values and the resulting rating for all scenarios. Additionally, all weights are default weights of $\omega = 1$.

TABLE 4 Expected input values and resulting ratings for the discussed scenarios.

Scenario	Load	Quality	Relevance	Trust	∑ V2X field
Highway	4	4	3	2	3
Rush hour	3	5	1	5	4
Parking lot	4	5	1	4	4

Weights ($\omega = 1$).

5.1. Highway Scenario

For this scenario, we expect a rural highway with sparse traffic where the only changing V2X traffic is caused by oncoming traffic. At 100 km/h, we can expect a vehicle to join our communication range every 10 s. With a perfect line of sight, we can expect a maximum single-hop communication range of around 400 m, according to Pilz et al. [16]. This means that one vehicle has around 30 s within the communication range. With this traffic density, one would have around four vehicles in the oncoming traffic lane and two in the ego lane in the direct communication range. According to specifications [2], the frequency for CAMs on the highway would be in the lower third of the 1–10 Hz range. The CPMs would be in the upper third of the 1–10 Hz range because of the rapidly changing positions of detected vehicles, according to specifications [3]. Hence, for our example, we can expect below 10 Hz of messages per ITS-S and 70 Hz in total for all surrounding ITS-Ss without packet loss. The packet loss will bring both numbers slightly down, which means the rating for the number of incoming messages per ITS-S is $R_{CL(msg)} = 3$, and per channel is $R_{CL(ch)} = 5$. The final rating is then $R_{CL} = ((7–1(3 * 7)) * 1 + 5 * 1)/(1 + 1) = 4$.

For the quality of information, we know that the localization accuracy has to be better than 1.4 m for highways, according to Reid et al. [36], and we also know that the accuracy for CPMs can be off 1.9 m at low speeds, according to Pilz et al. [12]. Both result in an accuracy rating of $R_{QI(acc)} = 3$. The rating for the age of information will be $R_{QI(age)} = 5$ because when the message is sent, it is recent, and there is no relevant transmission delay in this scenario, according to Pilz et al. [16]. The final rating is $R_{QI} = (3 * 1 + 5 * 1)/2 = 4$.

For the relevance of information, we have distances up to 400 m due to the distances in this scenario. The average rating of the information of all seven vehicles is $R_{RI(dist)} = 4$. For the novelty of information, one can see that multiple CPMs will confirm the position of vehicles among each other. CPM redundancy specifications [3] will cause better novelty of information but also a higher age of information. Higher CPM frequencies will lead to more loaded channels and packet loss, as shown in this work. Hence, a novelty rating of around $R_{RI(novel)} = 2$ is applicable. The final rating is $R_{RI} = (4 * 1 + 2 * 1)/2 = 3$.

For the trustworthiness of information, we expect a rating of $R_{TI(src)} = 3$ for trustworthy sources. Onboard the

ego vehicle, we can only process the signature of incoming messages. Everything else needs a backend system that is not yet available. For the data itself, we can either put $R_{TI(data)} = 0$ because there is too little traffic to confirm the positions of vehicles, or we can put $R_{TI(data)} = 1$ because there are too few stations to confirm the data. To engage in a discussion, we do the latter. The final rating is $R_{TI} = (2 * 1 + 1 * 1)/2 = 2$.

The overall final rating is now $R = (4 * 1 + 4 * 1 + 3 * 1 + 2 * 1)/4 = 3$. One can see from the process of acquiring this rating that multiple incoming sources must be considered. Each message within the time for calculation needs a separate rating. Our example puts it easy and estimates a rough outline. One can also see that the rating should be driving situation dependent. As we drive on the highway, e.g., the novelty of information may be rated differently. Also, the configuration of importance weights for the ratings may change the trustworthiness of information down to $R_{TI} = 1$.

5.2. Rush Hour Scenario

In this scenario, we expect a traffic jam or slow traffic during rush hour in a bigger city like Vienna, Austria. We have a road with four lanes in one direction, toward an intersection crossing a similar road. There are hardly any pedestrians because it is an industrial area. Furthermore, as it is a city scenario, we can expect less range due to obstructions, as Pilz et al. showed [16]. Still, the ITS-Ss will reduce the overall transmission power, according to the standard [38].

We can expect each ITS-S to send hardly any messages due to the specifications in channel load scenarios [38] and the low speed [2]. Hence, the CAMs are down to around 1 Hz per vehicle. The CPMs will also be on the lower end according to the standard [3] because vehicles are not moving, and there are hardly any pedestrians on the main traffic way. The rating of incoming messages for all ITS-Ss is $R_{CL(msg)} = 1$. The rating for the overall channel load now also depends on the interpretation. In such a scenario, the regulations for message generation of CAMs and CPMs and the transmission power reduction may allow a channel load rating of $R_{CL(ch)} = 4$. However, this may drastically change if people walk between vehicles, as this would be considered dangerous and important, to which extent multiple vehicles would increase the transmission of messages, according to specifications [3]. The final channel rating is $R_{CL} = (1 + 4)/2 = 3$.

According to Pilz et al. [12], we can expect highly accurate data at a standstill and at low speeds for the quality of information. Also, the age of information can be expected to be low with the above channel expectations and field results gathered in this article. Hence, the final quality rating is $R_{QI} = (5 + 5)/2 = 5$.

For the relevance of information, we can expect a low rating of $R_{RI(dist)} = 1$ for the distance of information, as most messages are received from surrounding vehicles in a range that onboard sensors could cover. The novelty of information will also be poor, as multiple vehicles detect each other, resulting in multiple updated surrounding objects. Even with CPM redundancy mitigation on each vehicle, one may expect a novelty of information rating of $R_{RI(novel)} = 1$. Hence, the final relevance of information rating is $R_{RI} = (1 * 1)/2 = 1$, which can be expected in a traffic jam.

Things can be expected to be ultimately the opposite for the trustworthiness rating. For the trustworthy sources, we can expect $R_{TI(src)} = 5$, as there is the chance to confirm messages of one vehicle multiple times, and other vehicles could confirm the trustworthiness of single sources. Similarly, the trustworthy data rating will be $R_{TI(data)} = 5$ in normal conditions because we can verify incoming data easily with cross-correlated information from other vehicles. Hence, the final trustworthiness rating is $R_{TI} = (5 + 5)/2 = 5$.

In this scenario, one can see that the weights have to be adapted for specific traffic situations. One can expect the quality of information to be high. However, the relevance of information should have a much higher impact on the overall rating, as the V2X-as-a-sensor information is mostly unnecessary computing overhead during rush hour. Digging deeper, the channel load itself is on a split. One should argue that the quality rating is more a 2 than a 3 because while the overall channel load is good, individuals have less capacity for the overall channel.

5.3. Parking Lot Scenario

In this scenario, we discuss the quality rating of the V2X field on a busy day at the shopping center's parking lot. Many objects, from vehicles to bicycles to pedestrians, are present, so the load of information is high. However, parked vehicles will not communicate in our scenario. Only the vehicles driving between the lanes and looking for a parking spot will.

We can expect rapid updates of 10 Hz for the channel load for CAMs as vehicles maneuver. We can also expect rapid updates of 10 Hz for CPMs, as pedestrians will be walking around, triggering the generation according to specifications [3]. Hence, the individual channel load rating is $R_{CL(msg)} = 5$, right in the optimal center. However, the overall channel load is most likely at $R_{CL(ch)} = 3$, up to around 20 vehicles, using the results of this work. Also, $R_{CL(ch)} = 2$ is realistic on a busy day. In both cases, the channel rating is $R_{CL} = 4$ with $R_{CL} = (5 + 3)/2 = 4$ and $R_{CL} = (5 + 2)/2 = 4$.

The quality of information is tricky. As shown by Pilz et al. [12], the accuracy of detected vehicles is low when the dimensions cannot be fully detected. Hence, the accuracy rating can be expected as $R_{QI(acc)} = 4$ on average. The age of information is dependent on the channel load. If CPMs starve in the sending queue, the age of information will increase. However, most messages will likely come through with low delay, as the channel is only half

full, leading to $R_{QI(age)} = 5$. Hence, the final quality of information rating is $R_{QI} = (4 + 5)/2 = 5$.

The relevance of information is similar to the rush hour scenario. The information distance is $R_{RI(dist)} = 1$, as most critical parking lot movement can be detected with onboard sensors. Also, the novelty of information is down at $R_{RI(novel)} = 1$ because pedestrian movement requires frequent updates of the position and heading, but the object itself is already known. Hence, the final relevance rating is $R_{RI} = (1 + 1)/2$.

The trustworthiness rating is again expected to be high. The trustworthiness of sources can be verified in multiple updates, as the ITS-Ss stay long in the communication range. This results in a rating of $R_{TI(src)} = 5$. The trustworthy data rating is also high because multiple vehicles confirm each other. However, due to several standstill vehicles parking between active vehicles, it is more likely that only a handful of vehicles can verify each other, leading to a rating of $R_{TI(data)} = 3$. Hence, the final trustworthy rating of $R_{TI} = (5 + 3)/2 = 4$.

The parking lot scenario is another good example of V2X-as-a-sensor. V2X can track traffic around the corner, such as open parking spots. But as one can see with the relevance of information rating, repeated information can be a downside. This scenario also shows that the weights for the overall V2X field rating inputs must be adapted for each use case. For example, individual channel loads may be more prominent, similar to the information age. Also, the novelty of information may be less relevant than the trustworthiness of information to guarantee the safety of pedestrians.

6. Discussion

This article tackled existing gaps in performance measurements and combined this insight with existing performance indicators to design a metric for assessing the quality of the surrounding V2X field.

Guided by the works of Pilz et al. [12, 16], this work first did a measurement campaign on loaded V2X channels to fill important gaps in performance. The test setups followed Pilz et al. [12, 16] to ensure comparability and extendibility. The results demonstrate the expectations toward the delay behavior in loaded channels, where delays >>100 ms should be expected. Previously, this data was only available from simulations and theoretical estimations, as discussed by Pilz et al. [16]. Additionally, this work demonstrated the increase of the FoV, which is a logical implication of CP and V2X-as-a-sensor in general but has not been discussed by the analysis and literature review of Pilz et al. [12] for its benefits.

Next, this article defined a metric to break down the performance of the surrounding V2X field into components and down to a single number, which an AD system can use to estimate the QoS. Till now, AD systems incorporated the V2X data into their system without being aware of the quality of the current data. Especially the domain of trustworthiness [8, 9, 10, 11] raised the question of the quality of provided data, followed by many other domains, as introduced in Section 1. The modularity of this metric allows the metric to be calculated in a distributed manner without the need for central tracking.

The separation also allows one to adapt the calculation of the V2X field quality with weights. These weights can be adapted to specific situations, as demonstrated in Section 5. From the discussed scenarios, one can see that specific scenarios have different requirements for the quality of the V2X field. Highway scenarios require a low delay, while parking lot scenarios require a high novelty of information.

Overall, this initial approach is a viable solution for most use cases. At its core, the metric should aid the discussions between the different approaches of the AD and V2X domains. The AD domain can now more easily deal with the varying quality of the wireless connection and V2X communication. In contrast, the V2X domain can now more reliably target the needs of AD systems.

Finally, the metric design discovered an open issue regarding integrating the FoV extension. Details about the sensor coverage and space occupancy are necessary to describe the quality of the FoV. Additional research has to be conducted for both indicators.

Seeing V2X-as-a-sensor only as an additional sensor helps to understand the downside of V2X. Because of many influence factors, the full mix of various sources may never provide a clear sensor image comparable to a camera or a lidar. However, this is exactly why this rating metric is needed and, hence, why future research has to find a way to rate the FoV and include these two performance indicators.

7. Conclusion

In this article, we designed a rating metric for the V2X field surrounding an AV. The V2X field rating aids an AD system in its decision on the usefulness of information in the surrounding V2X field. The rating incorporates the most important influencing factors, from the channel's throughput over the quality and relevance of information to the trustworthiness of the sources and data.

Before the design process, we collected additional necessary measurements to fill gaps from related research on loaded channels. We also provided a set of FoV measurements to show the usefulness of extending the FoV with V2X-as-a-sensor.

The design process combined previous and related research know-how with new and additional insight into specific research gaps. Most prominently, we discussed the shape of the rating for each specific component. This shape was modeled as straightforwardly as possible onto the minima, maxima, and expected behavior, which are, in turn, provided by previous and related research.

We then discussed the overall metric's expressiveness using three core examples. We thereby highlighted the single metrics' expressiveness and the possibility that tuning the weights for specific driving situations may provide even better insight into the current state of the V2X field.

Finally, we discussed the flow of information when creating the metric. We highlighted the rating metric's benefits and open issues, especially the missing metric for evaluating the quality of the provided FoV.

For future research, we see the need to integrate this metric into a complex simulation environment that can simulate both V2X data exchange, such as CP information, and the behavior of the wireless network. This integration could render ready-to-use blocks, such as ROS nodes, to be shared within the community. Simulation datasets and ready-to-use building blocks would, in turn, foster research on the tuning of rating weights, which would allow a discussion on the importance of specific QoS parameters for specific driving scenarios.

Our research team is also looking forward to setting up a V2X environment on campus that allows us to evaluate the metric more fully in real life. Combined with parallel simulation studies, this could lead to a more widespread application of the rating metric and probably even an introduction to the standardization of ETSI. Certain QoS ratings could even be provided within the V2X message.

From its current stance, the V2X rating metric is one-dimensional. Stepping up to a second dimension, the V2X field rating could integrate the FoV rating more easily. As discussed, the FoV rating has to deal with sensor coverage and occupancy. By making the V2X field rating two-dimensional, one could introduce several factors in 1 × 1-m squares and have better ratings for spaces where FoV inputs overlap, creating an occupancy-like grid.

Acknowledgements

The research leading to these results/this publication has received funding from the European Union's Horizon Europe research and innovation programme under grant agreement No 101069748—SELFY project. Views and opinions expressed are, however, those of the author(s) only and do not necessarily reflect those of the European Union or CINEA. Neither the European Union nor the granting authority can be held responsible for them will be added after the double-blind phase, as requested.

The publication was written at Virtual Vehicle Research GmbH in Graz and partially funded by the COMET K2 Competence Centers for Excellent Technologies from the Austrian Federal Ministry for Climate Action (BMK), the Austrian Federal Ministry for Digital and Economic Affairs (BMDW), the Province of Styria (Dept. 12), and the Styrian Business Promotion Agency (SFG). The Austrian Research Promotion Agency (FFG) has been authorized for the programme management.

Contact Information

Christoph Pilz, corresponding author
c.pilz@student.tugraz.at
christoph.pilz@v2c2.at
c.pilz@ymail.com

CRediT Author Statement

Christoph Pilz: Conceptualization, investigation, software, and writing

Lukas Kuschnig: Software, conceptualization, resources, writing original draft

Alina Steinberger: Software, data curation

Peter Sammer: Resources, software

Esa Piri: Data curation, formal analysis, methodology, writing original draft

Christophe Couturier: Data curation, formal analysis, writing original draft

Thomas Neumayr: Software

Markus Schratter: Software, resources

Gerald Steinbauer-Wagner: Supervision

Abbreviations

AD - Automated Driving
ADD - Automated Driving Demonstrator
AI - Artificial Intelligence
AV - Automated Vehicle
CA - Cooperative Awareness
CAM - CA Message
CBR - Channel Busy Ratio
CCAM - Cooperative Connected Automated Mobility
CP - Collective Perception
CPM - CP Message
CSMA/CA - Carrier Sense Multiple Access with Collision Avoidance
DCC - Decentralized Congestion Control
DEN - Decentralized Environmental Notification
DENM - DEN Message
EDCA - Enhanced Distribution Channel Access

FOSS - Free and Open-Source Software
FoV - Field of View
GN - Geographical Networking
ITS - Intelligent Transport Systems
ITSG5 - Intelligent Transport Systems in the 5GHz band
ITS-S - ITS Station
PLR - Packet Loss Ratio
QoS - Quality of Service
RSSI - Received Signal Strength Indication
V2X - Vehicle to Everything
ZMQ - Zero Message Queueing

References

1. ETSI, "Intelligent Transport System (ITS); Vehicular Communications; Basic Set of Applications; Part 3: Specifications of Decentralized Environmental Notification Basic Service," ETSI EN 302 637-3 V1.2.1 (Final Draft), 2014.
2. ETSI, "Intelligent Transport Systems (ITS); Vehicular Communications; Basic Set of Applications; Part 2: Specification of Cooperative Awareness Basic Service," ETSI EN 302 637-2 V1.3.1, 2014.
3. ETSI, "Intelligent Transport System (ITS); Vehicular Communications; Basic Set of Applications; Specification of the Collective Perception Service, Release 2," ETSI TS 103 324 V0.0.52 (Draft), 2022.
4. Lang, U. and Schreiner, R., "Managing Security in Intelligent Transport Systems," in *Proceedings of the 2015 IEEE 18th International Conference on Intelligent Transportation Systems*, Gran Canaria, Spain, 2015, 48-53, https://doi.org/10.1109/ITSC.2015.16.
5. Škorput, P., Vojvodić, H., and Mandžuka, S., "Cyber Security in Cooperative Intelligent Transportation Systems," in *Proceedings of the 2017 International Symposium ELMAR*, Zadar, Croatia, 2017, 35-38, https://doi.org/10.23919/ELMAR.2017.8124429.
6. Harvey, J. and Kumar, S., "A Survey of Intelligent Transportation Systems Security: Challenges and Solutions," in *Proceedings of the 2020 IEEE 6th Intl Conference on Big Data Security on Cloud (BigDataSecurity), IEEE Intl Conference on High Performance and Smart Computing, (HPSC) and IEEE Intl Conference on Intelligent Data and Security (IDS)*, Baltimore, MD, 2020, 263-268, https://doi.org/10.1109/BigDataSecurity-HPSC-IDS49724.2020.00055.
7. Ansari, M.R., Monteuuis, J.P., Petit, J., and Chen, C., "V2X Misbehavior and Collective Perception Service: Considerations for Standardization," in *Proceedings of the 2021 IEEE Conference on Standards for Communications and Networking (CSCN)*, Thessaloniki, Greece, 2021, 1-6, https://doi.org/10.1109/CSCN53733.2021.9686156.
8. Allig, C., Leinmüller, T., Mittal, P., and Wanielik, G., "Trustworthiness Estimation of Entities within Collective Perception," in *Proceedings of the 2019 IEEE Vehicular Networking Conference (VNC)*, Los Angeles, CA, 2019, 1-8, https://doi.org/10.1109/VNC48660.2019.9062796.
9. Hurl, B., Cohen, R., Czarnecki, K., and Waslander, S., "TruPercept: Trust Modelling for Autonomous Vehicle Cooperative Perception from Synthetic Data," in *Proceedings of the 2020 IEEE Intelligent Vehicles Symposium (IV)*, Las Vegas, NV, 2020, 341-347, https://doi.org/10.1109/IV47402.2020.9304695.
10. Shoker, A., Moertl, P., and Robles, R., "A First Step towards Holistic Trustworthy Platoons," in *Proceedings of the 2021 IEEE 7th World Forum on Internet of Things (WF-IoT)*, New Orleans, LA, 2021, 795-800, https://doi.org/10.1109/WF-IoT51360.2021.9595496.
11. Michalopoulos, P., Meijers, J., Singh, S.F., and Veneris, A., "A V2X Reputation System with Privacy Considerations," in *Proceedings of the 2022 IEEE 13th International Conference on Software Engineering and Service Science (ICSESS)*, Beijing, China, 2022, 8-14, https://doi.org/10.1109/ICSESS54813.2022.9930178.
12. Pilz, C., Steinberger, A., and Steinbauer-Wagner, G., "Positional Accuracy Provided by State-of-the-Art Cooperative Awareness and Collective Perception," in *Proceedings of the 2023 IEEE International Intelligent Transportation Systems Conference (ITSC)*, Bilbao, Spain, 2023.
13. Hoiem, D., Chodpathumwan, Y., and Dai, Q., "Diagnosing Error in Object Detectors," in Fitzgibbon, A., Lazebnik, S., Perona, P., Sato, Y. et al. (eds.), *Proceedings of the Computer Vision—ECCV 2012* (Berlin, Heidelberg: Springer, 2012), 340-353.
14. Wenkel, S., Alhazmi, K., Liiv, T., Alrshoud, S. et al., "Confidence Score: The Forgotten Dimension of Object Detection Performance Evaluation," *Sensors* 21 (2021): 4350, doi:https://doi.org/10.3390/s21134350.
15. Miller, D., Moghadam, P., Cox, M., Wildie, M. et al., "What's in the Black Box? The False Negative Mechanisms inside Object Detectors," *IEEE Robotics and Automation Letters* 7 (2022): 8510-8517, doi:https://doi.org/10.1109/LRA.2022.3187831.
16. Pilz, C., Sammer, P., Piri, E., Grossschedl, U. et al., "Collective Perception: A Delay Evaluation with a Short Discussion on Channel Load," *IEEE Open Journal of Intelligent Transportation Systems* 4 (2023): 506-526, doi:https://doi.org/10.1109/OJITS.2023.3296812.
17. Harkat, Y. and Amrouche, A., "Vehicle Density, Vehicle Speed and Packet Inter-Arrival Time Analysis in IEEE 802.11p EDCA Based VANETs," in *Proceedings of the 2018 International Conference on Signal, Image, Vision and Their Applications (SIVA)*, Guelma, Algeria, 2018, 1-6, https://doi.org/10.1109/SIVA.2018.8661070.
18. Zheng, J. and Wu, Q., "Performance Modeling and Analysis of the IEEE 802.11p EDCA Mechanism for VANET," *IEEE Transactions on Vehicular Technology* 65

(2016): 2673-2687, doi:https://doi.org/10.1109/TVT.2015.2425960.

19. Sun, W., Zhang, H., Pan, C., and Yang, J., "Analytical Study of the IEEE 802.11p EDCA Mechanism," in *Proceedings of the 2013 IEEE Intelligent Vehicles Symposium (IV)*, Gold Coast, QLD, Australia, 2013, 1428-1433, https://doi.org/10.1109/IVS.2013.6629667.
20. Engelstad, P. and Osterbo, O., "Delay and Throughput Analysis of IEEE 802.11e EDCA with Starvation Prediction," in *Proceedings of the IEEE Conference on Local Computer Networks 30th Anniversary (LCN'05)*, Sydney, NSW, Australia, 2005, 647-655, https://doi.org/10.1109/LCN.2005.47.
21. Huang, H., Li, H., Shao, C., Sun, T. et al., "Data Redundancy Mitigation in V2X Based Collective Perceptions," *IEEE Access* 8 (2020): 13405-13418, doi:https://doi.org/10.1109/ACCESS.2020.2965552.
22. Delooz, Q. and Festag, A., "Network Load Adaptation for Collective Perception in V2X Communications," in *Proceedings of the 2019 IEEE International Conference on Connected Vehicles and Expo (ICCVE)*, Graz, Austria, 2019, 1-6, https://doi.org/10.1109/ICCVE45908.2019.8964988.
23. Thandavarayan, G., Sepulcre, M., and Gozalvez, J., "Generation of Cooperative Perception Messages for Connected and Automated Vehicles," *IEEE Transactions on Vehicular Technology* 69 (2020): 16336-16341, doi:https://doi.org/10.1109/TVT.2020.3036165.
24. Aoki, S., Higuchi, T., and Altintas, O., "Cooperative Perception with Deep Reinforcement Learning for Connected Vehicles," in *Proceedings of the 2020 IEEE Intelligent Vehicles Symposium (IV)*, Las Vegas, NV, 2020, 328-334, https://doi.org/10.1109/IV47402.2020.9304570.
25. Abdel-Aziz, M.K., Perfecto, C., Samarakoon, S., Bennis, M. et al., "Vehicular Cooperative Perception through Action Branching and Federated Reinforcement Learning," *IEEE Transactions on Communications* 70 (2022): 891-903, doi:https://doi.org/10.1109/TCOMM.2021.3126650.
26. Ghnaya, I., Ahmed, T., Mosbah, M., and Aniss, H., "Maximizing Information Usefulness in Vehicular CP Networks Using Actor-Critic Reinforcement Learning," in *Proceedings of the 2022 18th International Conference on Network and Service Management (CNSM)*, Thessaloniki, Greece, 2022, 296-302, https://doi.org/10.23919/CNSM55787.2022.9964740.
27. Delooz, Q., Willecke, A., Garlichs, K., Hagau, A.-C. et al., "Analysis and Evaluation of Information Redundancy Mitigation for V2X Collective Perception," *IEEE Access* 10 (2022): 47076-47093, doi:https://doi.org/10.1109/ACCESS.2022.3170029.
28. Shahen Shah, A.F.M., Ilhan, H., and Tureli, U., "Modeling and Performance Analysis of the IEEE 802.11P MAC for VANETs," in *Proceedings of the 2019 42nd International Conference on Telecommunications and Signal Processing (TSP)*, Budapest, Hungary, 2019, 393-396, https://doi.org/10.1109/TSP.2019.8769073.
29. Septa, N., "The Performance Analysis of 802.11p with Cooperative Communication and Dynamic Contention Window," *Wireless Personal Communications* 131 (2023): 431-454, doi:https://doi.org/10.1007/s11277-023-10437-w.
30. Pilz, C., Ulbel, A., and Steinbauer-Wagner, G., "The Components of Cooperative Perception—A Proposal for Future Works," in *Proceedings of the 2021 IEEE International Intelligent Transportation Systems Conference (ITSC)*, Indianapolis, IN, 2021, 7-14, https://doi.org/10.1109/ITSC48978.2021.9564989.
31. Cui, G., Zhang, W., Xiao, Y., Yao, L. et al., "Cooperative Perception Technology of Autonomous Driving in the Internet of Vehicles Environment: A Review," *Sensors* 22 (2022): 5535, doi:https://doi.org/10.3390/s22155535.
32. Karner, M., Peltola, J., Jerne, M., Kulas, L. et al., *Intelligent Secure Trustable Things* (Cham, Switzerland: Springer International Publishing, 2024)
33. Pilz, C., Neubauer, P., Steinberger, A., and Krizanec, N., "Vehicle Communication Platform to Anything—Toolbox," 2023, last visited February 13, 2023.
34. Saarinen, J., Andreasson, H., Stoyanov, T., and Lilienthal, A.J., "Normal Distributions Transform Monte-Carlo Localization (NDT-MCL)," in *Proceedings of the 2013 IEEE/RSJ International Conference on Intelligent Robots and Systems*, Tokyo, Japan, 2013, 382-389, https://doi.org/10.1109/IROS.2013.6696380.
35. ETSI, "Intelligent Transport Systems (ITS); Decentralized Congestion Control Mechanisms for Intelligent Transport Systems Operating in the 5 GHz Range; Access Layer Part," ETSI TS 102 687 V1.2.1, 2018.
36. Reid, T., Houts, S., Cammarata, R., Mills, G. et al., "Localization Requirements for Autonomous Vehicles," *Conference: Society of Automotive Engineers World Congress Experience* 2 (2019): 173-190, doi:https://doi.org/10.4271/12-02-03-0012.
37. Yates, R.D., Sun, Y., Brown, D.R., Kaul, S.K. et al., "Age of Information: An Introduction and Survey," *IEEE Journal on Selected Areas in Communications* 39 (2021): 1183-1210, doi:https://doi.org/10.1109/JSAC.2021.3065072.
38. ETSI, "Intelligent Transport Systems (ITS); STDMA Recommended Parameters and Settings for Cooperative ITS; Access Layer Part," ETSI TR 102 861 V1.1.1. 832, 2012.